Challenge Journal of CONCRETE RESEARCH LETTERS

Vol.8 No.1 (2017)

CFRP acidic environment acoustic emission compressive strength concrete corrosion cracking ductility durability ferrocement fly ash mechanical properties palm oil fuel ash reinforced concrete self-compacting concrete silica fume steel mesh strength strengthening superplasticizer water a[illegible]ion

ISSN 2548-0928

TULPAR ACADEMIC PUBLISHING

Challenge Journal of Concrete Research Letters

EDITOR IN CHIEF

Prof. Dr. Mohamed Abdelkader ISMAIL	*Curtin University Sarawak, Malaysia*

EDITORIAL ADVISORY BOARD

Prof. Dr. Abdullah SAAND	*Quaid-e-Awam University of Engineering, Pakistan*
Prof. Dr. Alexander-Dimitrios George TSONOS	*Aristotle University of Thessaloniki, Greece*
Prof. Dr. Ashraf Ragab MOHAMED	*Alexandria University, Egypt*
Prof. Dr. Ayman NASSIF	*University of Portsmouth, United Kingdom*
Prof. Dr. Gamal Elsayed ABDELAZIZ	*Benha University, Egypt*
Prof. Dr. Hamidah Mohd SAMAN	*Universiti Teknologi Mara, Malaysia*
Prof. Dr. Han Seung LEE	*Hanyang University, Republic of Korea*
Prof. Dr. Zubair AHMED	*Mehran University, Pakistan*
Dr. Aamer Rafique BHUTTA	*Universiti Teknologi Malaysia, Malaysia*
Dr. Khairunisa MUTHUSAMY	*Universiti Malaysia Pahang, Malaysia*
Dr. Mahmoud SAYED AHMED	*Ryerson University, Canada*

E-mail: *cjcrl@challengejournal.com*

Web page: *cjcrl.challengejournal.com*

TULPAR Academic Publishing
www.tulparpublishing.com

Challenge Journal of Concrete Research Letters

CONTENTS

TULPAR ACADEMIC PUBLISHING

Challenge Journal of Concrete Research Letters

Comparative study on the using of PEG and PAM as curing agents for self-curing concrete

Alaa A. Bashandy *, Nageh N. Meleka, Mohamed M. Hamad

Department of Civil Engineering, Menoufia University, Shebin ElKoum, Menofia, Egypt

ABSTRACT

There are many factors, which may affect on concrete quality. One of those is concrete curing. Self-curing concrete is the solution. It may produce by using chemical curing agents. The concept of those agents is to reduce the water evaporation from concrete. This research aims to study the effect of chemical curing agents on the behavior of self-curing concrete. Two different chemical curing agents were used to study the main mechanical properties of concrete. The main variables are; the type of curing agent (Polyethylene glycol "PEG400"–Poly Acrylamide "PAM") and its dosages. The results obtained in terms of compressive, tensile and flexure strength values. Test results showed that the self-curing concrete cured by each agent performed better in hardened properties compared to none cured concrete. Also, curing using the both agents together perform better than using each one individually.

ARTICLE INFO

Article history:
Received 22 October 2016
Revised 23 January 2017
Accepted 11 March 2017

Keywords:
Self-curing concrete
Polyethylene glycol
PEG 400
Polyacrylamide
PAM

1. Introduction

The curing of concrete is an essential step in the concrete construction. A suitable curing period is essential at early ages to enable the concrete to have strength, to reduce shrinkage, and to develop a structure that will make the concrete sufficiently durable (Schlitter et al., 2010). Curing is the process by which hydraulic cement concrete develops hardened properties over time. Hardening of concrete is a result of the continued hydration of the cement in the presence of sufficient water and heat (ACI.308R–01, 2001). Water is necessary to the hydration reaction of the cement, which led the gray cement powder to convert into the binding cement paste, which gives concrete its strength (ACI.308R–01, 2001; Ambily and Rajamane, 2007). Excessive evaporation of water (internal or external) from fresh concrete led to unsatisfactory properties if it is not avoided. Curing regimes should ensure the availability of adequate amount of water for cement hydration.

Using self-curing "SC" concrete is a good solution to avoid the conventional curing processes (Jensen and Lura, 2006; Schlitter et al., 2010; Jagannadha Kumar et al., 2012; Junaid et al., 2015). It has satisfied characteristics in strength and durability (Dhir et al., 1995; Mather, 2001; Jagannadha Kumar et al., 2012; Kholia et al., 2013; Mousa et al., 2014; Vyawahare and Patil, 2014; Junaid et al., 2015; Bashandy, 2016). Also, SC concrete behaves well at elevated temperatures (Bashandy, 2015). The main idea of self-curing concrete is to cure the concrete from inside to outside. There are two main methods to obtain self-curing concrete (Chella-Gifta et al., 2013). The first is conducted by using porous materials (Lightweight Aggregates, Wood powder) to act as internal reservoirs (Bentur et al., 2001; Kovler et al., 2002; Ambily and Rajamane, 2007). The second is conducted by using chemical curing agents (Super-absorbent Polymers "SAP" and Shrinkage Reducing Admixture "SRA" such as polyethylene-glycol "PEG", polyacrylamide "PAM" and propylene glycol) (El Dieb et al., 2012; Sathanandham et al., 2013). Using PEGs results in self-curing, helps in better hydration, and improves strength (Sathanandham et al., 2013). Also, PEGs reduces early age shrinkage cracks. Adding PEGs to concrete led to forming shells around water particles. Those shells formed on every water particles present in the concrete with thicknesses of about 2nm. Due to the formation of those shells, water is not able to evaporate from concrete. That led to reduces rate

* *Corresponding author*. E-mail address: dr.alaa.bashandy@sh-eng.menofia.edu.eg (A. A. Bashandy)
ISSN: 2548-0928 / DOI: https://doi.org/10.20528/cjcrl.2017.01.001

of evaporation so water is always available at the time when hydration heat is going on. As evaporation does not take place there is no need for curing water (El Dieb, 2007; Sathanandham et al., 2013). PAM increases the strengths of concrete through its functions of absorbing water, filling larger pores, forming polymer films over hydrates, and interacting with hydration process (Rai and Singh, 2005). There are several types of SRAs. Each type of SRA has a different effect on the behavior of the obtained SC concrete (Jensen and Lura, 2006; El Dieb et al., 2012; Sathanandham et al., 2013; Kamal et al., 2016).

2. Research Significance

This research aims to investigate the effect of using two different chemical self-curing agents (PEG400 - PAM) on the hardened properties of concrete in order to obtain self-curing concrete. The main variables are; the type of self-curing agent (PEG400 - PAM) and the dosages of self-curing agents.

The importance of this research is to addressing the behavior of SC concrete for the researchers and engineers to overcome the possible problems due to insufficient curing. Fig. 1 shows the flow chart of the experimental program.

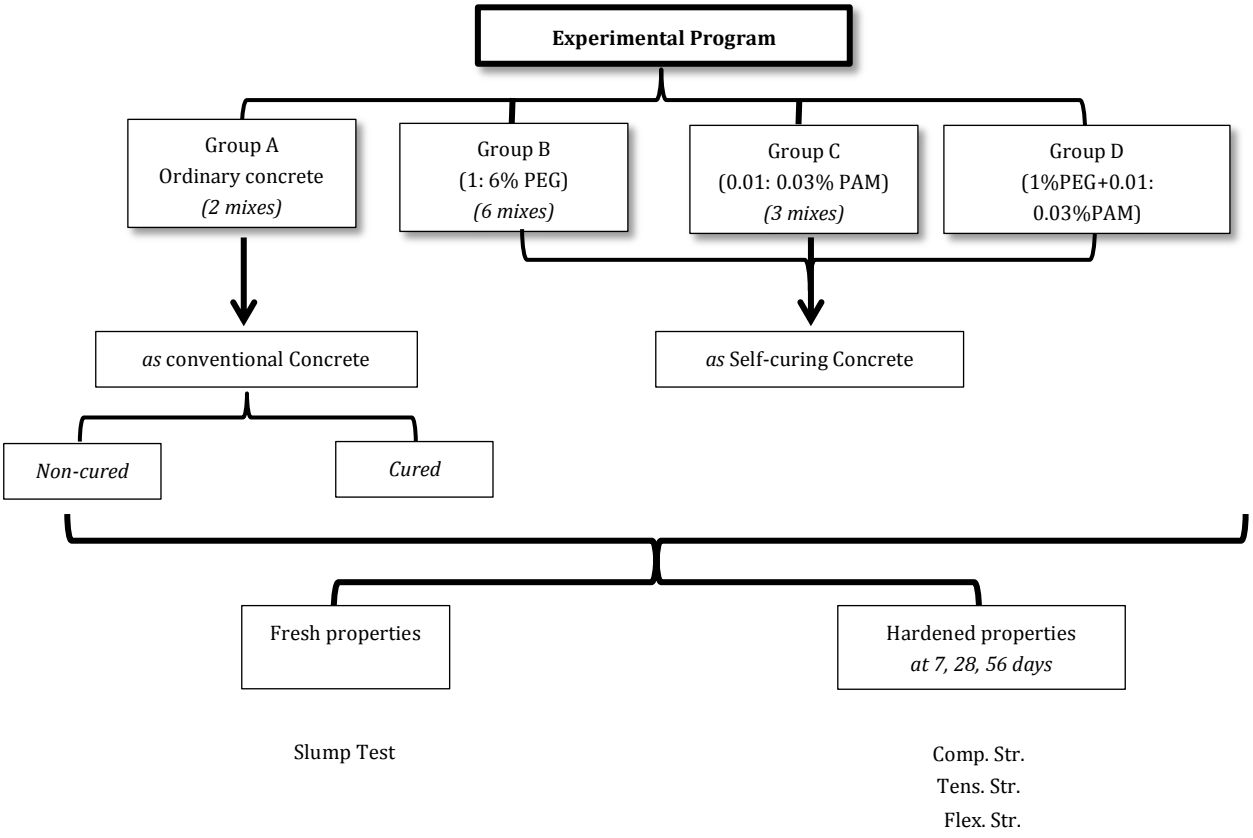

Fig. 1. Flow chart of experimental program.

3. Materials and Test Specimens

All tests in this research were carried out in the concrete research laboratory at Civil Eng. Dep. at Faculty of Engineering, Menoufia University.

The materials used, the design of test specimens and testing procedures are discussed in the following sections.

3.1. Materials

The cement used is ordinary Portland cement CEM I 42.5 N obtained from Lafarge factory. It satisfies the Egyptian Standard Specification (E.S.S. 4756-1/2009). Chemical and physical properties are shown in Table 1.

The fine aggregate used is natural siliceous sand that satisfies the Egyptian standards (E.S.S. 1109/2008). It is clean and nearly free from impurities with a specific gravity of 2.64 and a fineness modulus of 3.05. Its mechanical and physical properties are shown in Table 2.

The coarse aggregates used is crushed dolomite with a maximum nominal size of 10 mm, which satisfies the (E.S.S 1109/2008). Its mechanical and physical properties are shown in Table 3.

Drinkable clean water, fresh and free from impurities was used for mixing and curing satisfying the Egyptian Code of Practice (E.C.P. 203/2007).

A Super plasticizer "SP"as a high range water reducer without retarding effect for concrete is used. It complies with ASTM C-494 type F. The technical data at 25˚C is shown in Table 4. Silica fume as a pozzolanic additive is used in powder form satisfied. Chemical and physical properties are shown in Table 5**.**

The self-curing agents used in this study are two types; Polyethylene glycol 400 "PEG 400"and Polyacrylamide "PAM". PEG 400 is in liquid form as chemical

self-curing agent. Sisco Research Laboratories Company, India, manufactures it. The main physical and chemical properties are shown in Table 6. The PAM used is manufactured by Yixing Bluwat Chemicals Co. Ltd., China. The main physical and chemical properties are shown in Table 7.

Table 1. Typical properties of ordinary Portland cement used.

Property		Value
Surface Area	(m^2/kg)	310.0
Setting Time Initial	(minutes)	150.0
Specific Weight	(t/m^3)	3.12
Compressive Strength:		
2 day	(N/mm^2)	20.0
28 day	(N/mm^2)	49.0
Sulfate	SO_3 (%)	2.9
Chloride	CL (%)	0.06
Alkali Eq.	Na_2O (%)	0.50
Tri-Calcium Silicate	C_3S (%)	55.0 : 65.0
Di-Calcium Silicate	C_2S (%)	15.0 to 25.0
Tri-Calcium Aluminate	C_3A (%)	7.0
Tetra-Calcium Aluminoferrite	C_4AF (%)	11.0

Table 2. Typical properties of silica fume used.

Property		Value
Surface Area	(m^2/kg)	15000
Specific Weight	(kg/m^3)	2200
Sulfate	SO_3 (%)	0.30
Silicon Dioxide	SiO_2 (%)	95.0
Aluminum Oxide	AL_2O_3 (%)	0.40
Iron Oxide	Fe_2O_3 (%)	0.60
Calcium Oxide	CaO (%)	0.20
Magnesium Oxide	MgO (%)	0.40

Table 3. Mechanical and physical properties of sand used (as obtained from tests).

Sieve Size	(mm)	4.75	2.00	1.18	0.60	0.25	0.15
Pass	(%)	98.18	81.14	61.61	39.07	13.79	0.66
Fineness Modulus				3.05			
Specific Gravity				2.64			
Volume Weight	(kg/m^3)			1675			
Dust by Weight	(%)			0.01			

Table 4. Main mechanical and physical properties of crushed dolomite used (as obtained from tests).

Sieve Size	(mm)	4.75	2.00	1.18	0.60	0.25	0.15
Pass	(%)	98.18	81.14	61.61	39.07	13.79	0.66
MNS*	(mm)			10			
Specific Gravity				2.58			
Volume Weight	(kg/m^3)			1610			
Absorption Percentage	(%)			1.0			

** MNS = Maximum nominal size*

Table 5. Main properties of Addicrete PVF (as provided by manufacturer).

Property	Value
Base	Naphthalene sulphonate
Appearance	Brown liquid
Density (at 25°C)	1.18 ± 0.01 kg/l
Chloride Content	Nil
Air Entrainment	Nil
Compatibility	All types of Portland cement

Table 6. Main properties of Polyethylene glycol (PEG 400) as curing agent type 1 (as provided by manufacturer).

Property	Value
Average Molecular Weight	380 - 420 g/mol
Viscosity at 20°C	85 - 105 cs
Acidity	0.05% (max)
Wt /ml at 20°C	1.120 - 1.126 gm

Table 7. Main properties of Polyacrylamide (PAM) as curing agent type 2 (as provideD by manufacturer).

Property	Value
Average Molecular Weight	9000000 g/mol
Appearance	White crystalline powder
Specific Gravity	0.75 (50% aq. sol.)
PH Value	5 – 7

3.2. Concrete manufacturing

The start point of choosing the proportions of self-curing concrete mixes was conducted firstly based on previous researches (Yehia, 2010; El Dieb et al., 2012). All components of the concrete mixture of all stages are the same except the type and the dosage of self-curing agent, which considered as the main variable. The mixture proportions are illustrated in Table 8.

The pozzolanic additive (silica fume) used to reduce the concrete permeability then subsequently the concrete mixing water evaporation decreased and retained in the concrete as the self-curing agent does.

Table 8. Proportions of concrete mixes used.

Mixture code	Self-Curing Agent (as % of C)		Cement Content	Water	F.A.	C.A.	Silica Fume (addition)	S.P.
	PEG	PAM	(kg/m³)	(kg/m³)	(kg/m³)	(kg/m³)	(as % of C)	(%)
NC	--	--	300	150	643	1193	15	0.70
TC	--	--						
SE1	1.0	--						
SE2	2.0	--						
SE3	3.0	--						
SE4	4.0	--						
SE5	5.0	--						
SE6	6.0	--						
SA1	--	0.01						
SA2	--	0.02						
SA3	--	0.03						
SEA1	1.0	0.01						
SEA2	1.0	0.02						
SEA3	1.0	0.03						

3.3. Concrete samples

The conducted experimental program divided to four groups as shown in Tables 8 and 9. The first group performed to study the hardened concrete properties for conventionally cured concrete compared to non-cured concrete. The second group was performed to study the effect of using PEG400 only as the self-curing agent by six varied dosages from 1.0 up to 6.0 % of cement weight to obtain SC concrete. The third group was performed to study the effect of using three different dosages from PAM only as 0.01 to 0.03% of cement weight to obtain SC concrete too. The fourth group was performed to study the effect of using a mix of PEG400 and PAM as a self-curing agent by three different dosages (1.0%PEG + 0.01: 0.03% PAM). Table 9 shows the mix code identification for each group, slump values, and hardened concrete properties.

For all groups, fresh properties obtained in term of slump value The standard cone of dimensions 100mm upper diameter, 200 mm bottom diameter and 300 mm height was used according to the Egyptian Code of Practice (E.C.P. 203/2007). The main mechanical properties obtained in terms of compressive, tensile and flexure strengths according to E.C.P. 203/2007. The specimens are cubes (10×10×10 cm) to obtained compressive strength, cylinder (10cm diameter, 20 cm height) to obtained indirect tensile strength, and prism (10×10×50cm) to obtained flexural strength. A compressive strength testing machine of 2000 kN capacity was used to obtain compressive strength, indirect tensile strength and bond strength. A flexure-testing machine of 100 kN capacity was used to obtain flexural strength values. Tests performed after 7, 28, and 56 days of cast date.

4. Test Results and Discussions

The results of this study derived in terms of slump test for fresh concrete and in terms of compressive strength, indirect tensile (splitting) strength, and flexure strength of the hardened concrete.

4.1. Effect of using (PEG 400) as self-curing agent

The slump test values increased when the dose of (PEG400) increased as shown in Table 9. The effect of using PEG400 on the mechanical properties of the hardened concrete second group is shown in Table 9 and Figs. 2-7.

The specimens which cured traditionally (immersed in water) as control specimens recorded a compressive strength of 33.18 MPa at 28 days. The optimum dosage of PEG is 4% in the specimens (SE4) with a compressive strength of 35.64 MPa at 28 days' tests. The specimens with PEG (SE4) records greater strengths at 28 days than control specimens by about 7.4%, 11.70%, and 3.80% respectively, for compressive strength, indirect tensile strength, and flexural strength. The strength of the specimens (SE4) greater than that recorded for none cured (NC) at age of 28 days by 37.80%, 38.70 % and 39.90% respectively, for compressive, indirect tensile and flexural strengths. The optimum compressive strength value obtained at a dosage of 4.0% PEG which nearly agreed with previous researches (Yehia, 2010; Emam, 2012). Compressive strength values of control specimens at age of 56 days increase by about 58.50% and 11.20% for (NC) and (SE4) specimens, respectively. That may because of the presence of silica fume in the concrete mixture, which improves the strength to the concrete at the later ages. Practically, the performance of concrete mix (SE4) is better than that of control specimens at age 56 days in the case of the presence of difficulties in curing processes in the field.

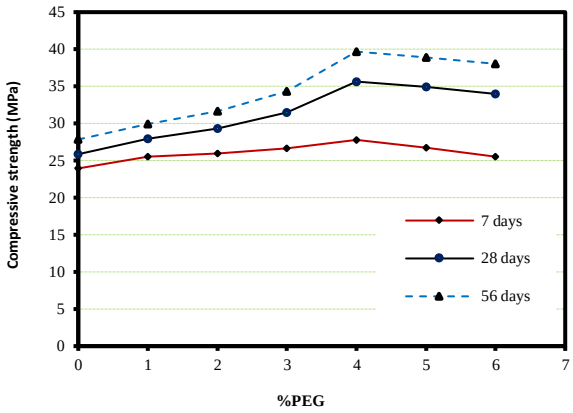

Fig. 2. Compressive strength values of the specimens versus the variable dosages of (PEG) as self-curing agent.

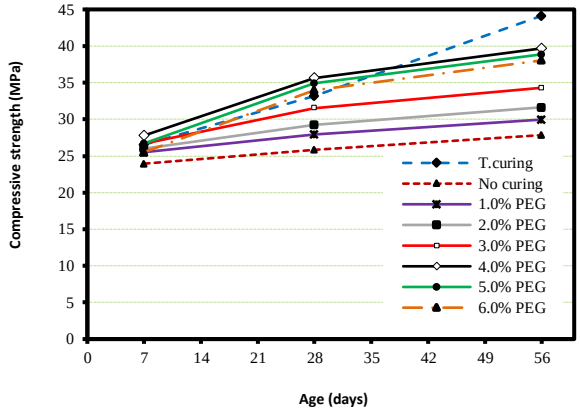

Fig. 3. Compressive strength values of concrete specimens cured by (PEG) as self-curing agent during early ages.

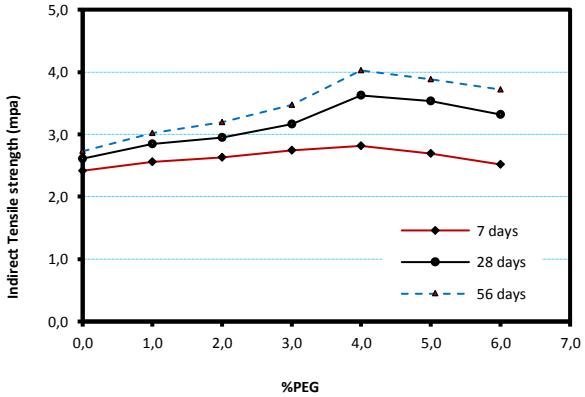

Fig. 4. Indirect tensile strength values of the specimens versus the variable dosages of (PEG) as self-curing agent.

Table 9. Concrete specimens and their main properties.

Group	Mix Code	Identification	Slump Test (mm)	Test Age (day)	Density (t/m³)	Comp-Strength (MPa)	Tensile Strength (MPa)	Flexural Strength (MPa)
A	TC	Traditional curing	56	7	2.50	26.54	2.62	2.73
				28	2.50	33.18	3.24	3.41
				56	2.48	44.13	4.22	4.50
	NC	Non -cured	56	7	2.46	23.94	2.42	2.31
				28	2.41	25.86	2.61	2.53
				56	2.36	27.84	2.73	2.76
B	SE1	Cured by 1% of cement weight PEG as self-curing agent of cement content	60	7	2.52	25.51	2.55	2.52
				28	2.52	27.91	2.85	2.82
				56	2.47	29.96	3.03	2.97
	SE2	PEG 2%	64	7	2.54	26.00	2.63	2.64
				28	2.52	29.28	2.95	3.00
				56	2.49	31.64	3.19	3.21
	SE3	PEG 3%	70	7	2.53	26.68	2.74	2.70
				28	2.52	31.52	3.17	3.20
				56	2.50	34.31	3.47	3.47
	SE4	PEG 4%	76	7	2.55	27.79	2.82	2.79
				28	2.52	35.64	3.62	3.54
				56	2.52	39.68	4.03	3.77
	SE5	PEG 5%	80	7	2.50	26.72	2.69	2.67
				28	2.50	34.95	3.53	3.49
				56	2.46	38.87	3.89	3.72
	SE6	PEG 6%	87	7	2.52	25.52	2.52	2.55
				28	2.50	33.95	3.32	3.34
				56	2.49	38.05	3.72	3.55
C	SA1	PAM 0.01%	55	7	2.53	26.85	2.78	2.55
				28	2.52	32.77	3.06	3.00
				56	2.50	33.53	3.40	3.24
	SA2	PAM 0.02%	49	7	2.49	24.45	2.50	2.40
				28	2.48	28.44	2.95	2.79
				56	2.48	29.11	3.25	3.06
	SA3	PAM 0.03%	45	7	2.45	20.74	2.20	2.01
				28	2.43	23.82	2.37	2.31
				56	2.40	24.22	2.51	2.55
D	SEA1	PEG+PAM 1.0%+0.01%	58	7	2.44	37.44	3.58	3.66
				28	2.42	44.86	4.46	4.35
				56	2.40	45.84	4.55	4.71
	SEA2	PEG+PAM 1.0%+0.02%	56	7	2.48	30.33	2.95	2.94
				28	2.46	43.17	4.22	3.84
				56	2.45	44.01	4.31	3.94
	SEA3	PEG+PAM 1.0%+0.03%	54	7	2.50	22.59	2.22	2.25
				28	2.48	25.10	2.47	2.46
				56	2.48	25.89	2.56	2.67

SE : Self-curing concrete mixture with Polyethylene glycol (PEG) as self-curing agent
SA : Self-curing concrete mixture with Polyacrylamide (PAM) as self-curing agent
SEA : Self-curing concrete mixture with combination of Polyethylene glycol +Polyacrylamide (PEG + PAM) as self-curing agent.

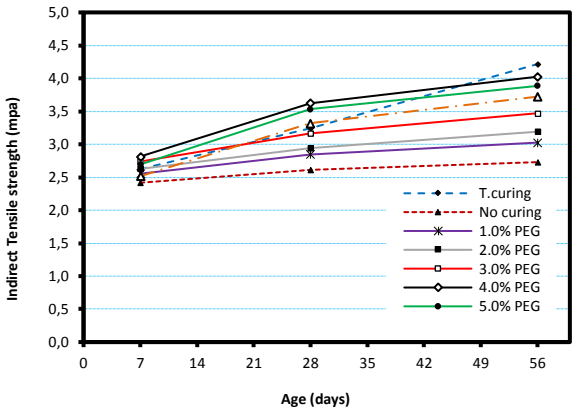

Fig. 5. Indirect tensile strength values of specimens cured by (PEG) as self-curing agent during early ages.

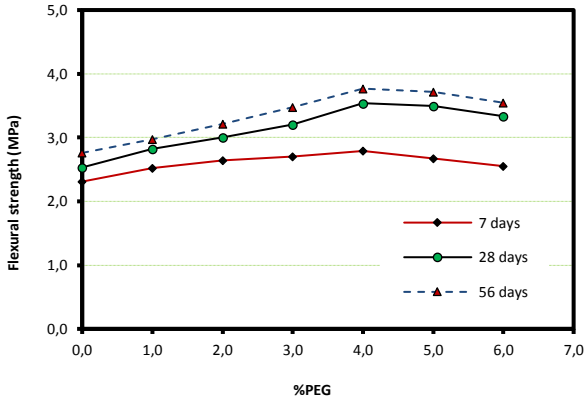

Fig. 6. Flexural strength values of the specimens versus the variable dosages of (PEG) as self-curing ages.

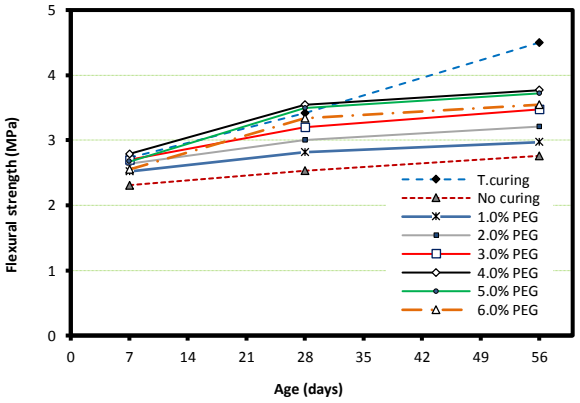

Fig. 7. Flexural strength values of concrete specimens cured by (PEG) as self-curing agent during early ages.

4.2. Effect of using (PAM) as self-curing agent

The slump test values (the fluidity) decreases initially, then increases, and decreases again with increasing PAM and the concrete mixture become sticky as shown in Table 9. That may because of the water-absorption effect of PAM, as well as the lubrication effect of the formed latex around cement particles (Sun and Xu, 2008). The effect of using PAM on the mechanical properties of hardened concrete (group C) are shown in Table 9 and Figs. 8-13. The optimum dosage of PAM is 0.01% (specimen SA1) which records a compressive strength value of 32.77 MPa at age of 28 days. The specimens cured by the optimum dosage of PAM (SA1) records strength less than control specimens (TC) at age of 28 days by 1.3%, 5.60% and 12%, respectively for compressive, indirect tensile and flexural strengths. The strength values of the specimens (SA1) are greater than that for none cured specimens (NC) at age of 28 days by about 26.70%, 17.24% and 18.57%, respectively for compressive, indirect tensile and flexural strengths. When the dosage of PAM increased more than 0.01% the strength of concrete decreased. It's noticed that the using of optimum dosage from PAM as self-curing agent in concrete specimens produced a compressive strength values less than that for cured by optimum dosage from PEG (SE4) by about 15.5 % at the age of 56 days and less than traditionally cured (TC) by 24% at the same age. That may results from the water-absorption effect of PAM compared to PEG.

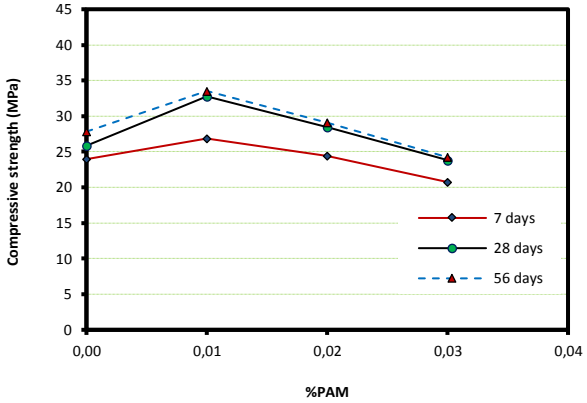

Fig. 8. Compressive strength values of the specimens versus the variable dosages of self-curing agent (PAM).

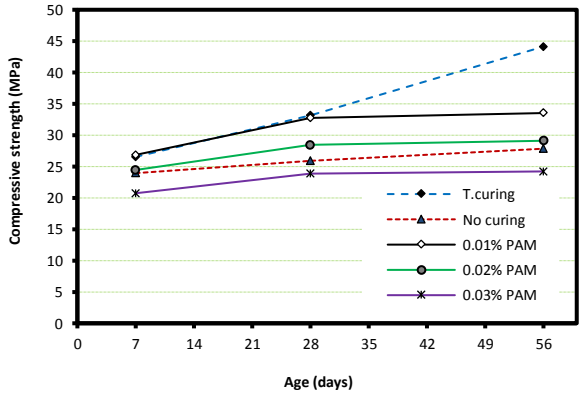

Fig. 9. Compressive strength values of concrete specimens cured by (PAM) as self-curing agent during early ages.

4.3. Effect of using a mix of PEG 400 and PAM as self-curing agents

The slump test values decreased when the dose of (PAM) increased as shown in Table 9. The effect of using a combination of both (as 1.0%PEG400 + PAM) on the mechanical properties of the hardened concrete (group D) are shown in Table 9 and Figs. 14-19.

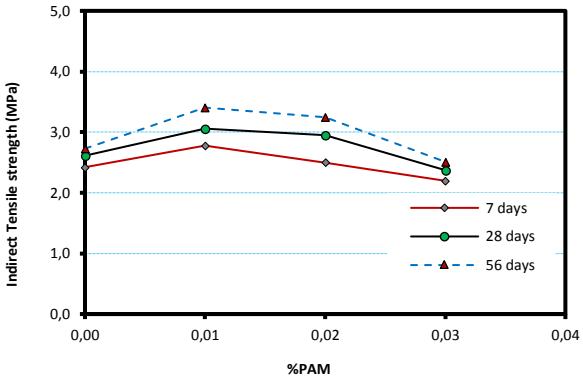

Fig. 10. Indirect tensile strength values of the specimens versus the variable dosages of (PAM) as self-curing agent.

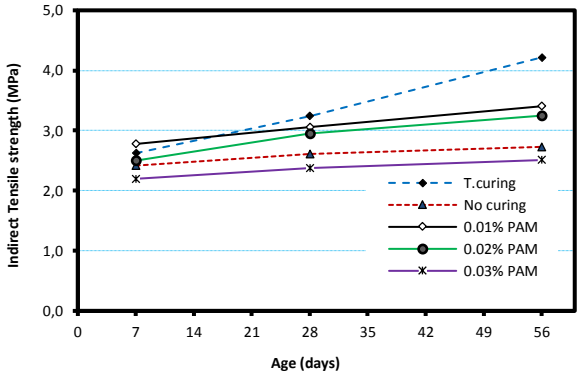

Fig. 11. Indirect tensile strength values of concrete specimens cured by (PAM) as self-curing agent during early ages.

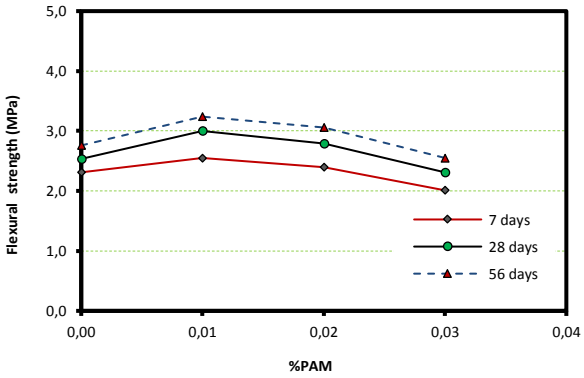

Fig. 12. Flexural strength values of the specimens versus the variable dosages of (PAM) as self-curing agent.

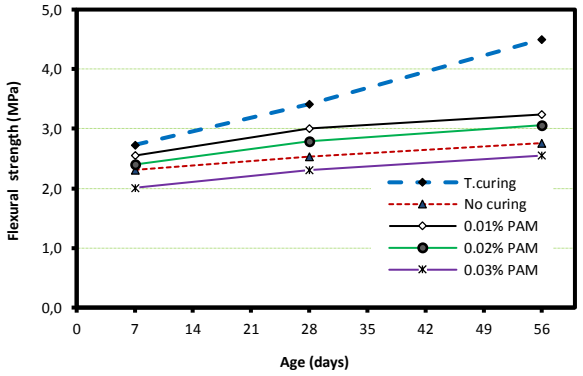

Fig. 13. Flexural strength values of all concrete specimens cured by (PAM) as self-curing agent during early ages.

The optimum dosage is at (0.01%PEG+0.01%PAM) in the specimens (SEA1) which records 44.86 MPa in compressive strength at age of 28 days. This specimen cured by the optimum dosage of the mixture (SEA1) records strength greater than control specimens (TC) at age of 28 days by 35.20%, 37.65% and 27.56%, respectively for compressive, indirect tensile and flexural strengths. The strength of the specimens (SEA1) is greater than that for none cured specimens (NC) at the age of 28 days by 73.47%, 70.88% and 71.93%, respectively for compressive, indirect tensile and flexural strengths.

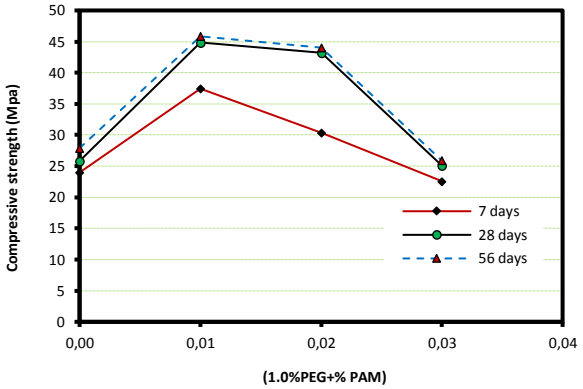

Fig. 14. Compressive strength values of the specimens at different dosages of (PEG+PAM) as self-curing agent.

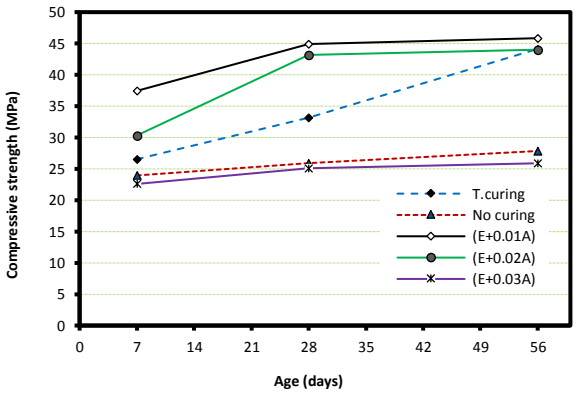

Fig. 15. Compressive strength values performance when cured using a mix of (PEG+PAM) as self-curing agent during early ages.

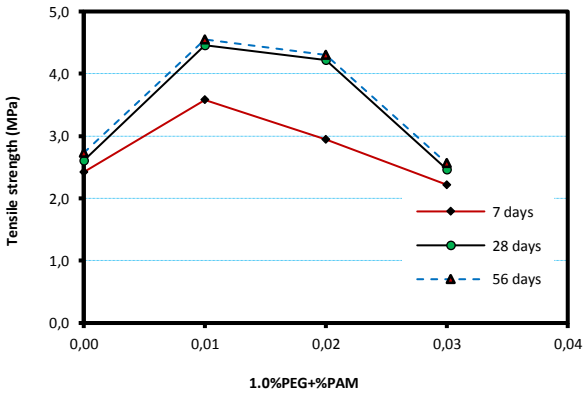

Fig. 16. Indirect tensile strength values of the specimens at different dosages of (PEG+PAM) as self-curing agent.

The compressive strength values decreased for dosages over 0.01% PAM at all ages. It is noticed that the using of optimum dosage from the mixture of (1.0%PEG400+PAM) as self-curing agent in concrete specimens gives compressive, indirect tensile, and flexure strength greater than that recorded for specimens cured by optimum dosage from PEG or PAM individually and greater than that traditionally cured also at all ages. That may result from the dual effect of each curing agent used which causes absorbing water, filling pores, forming polymer films over hydrates, and interacting with hydration process.

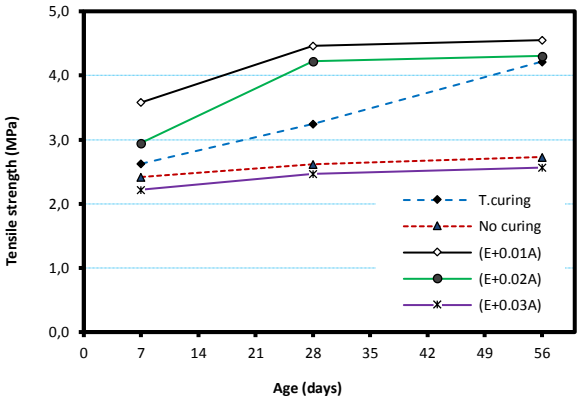

Fig. 17. Indirect tensile strength values when cured using a mix of (PEG+PAM) as self-curing agent during early ages.

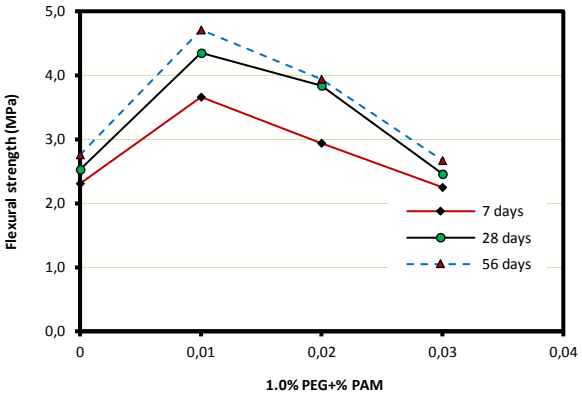

Fig. 18. Flexure strength values of the specimens at different dosages of (PEG+PAM) as self-curing agent.

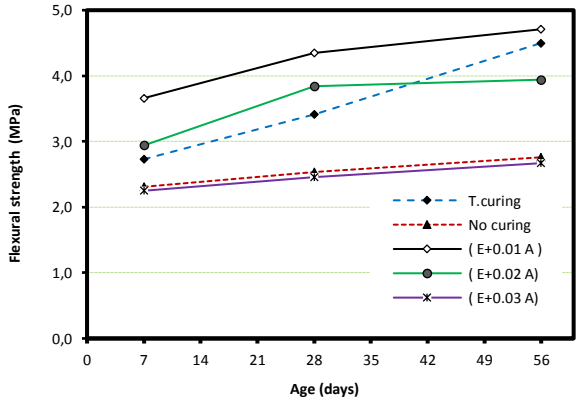

Fig. 19. Flexural strength values when cured using a mix of (PEG+PAM) as self-curing agent during early ages.

5. Conclusions

In this study, a series of experiments has been performed to investigate the behaviour and the properties of self-curing concrete specimens that cured by chemical self-curing admixtures. Comparison between self-curing concrete, traditional (cured in water), and none cured concrete has been done. Based on the experimental results presented in this paper, the conclusions could be drawn as follow:

- Using PEG400 or PAM is efficient to obtain SC concrete (in the range of this study).
- The slump values increased as increasing the content of PEG 400 while the slump values decreased as increasing the PAM content (in the range of this study).
- The optimum dosage when using PEG400 is 4% of cement content to obtain SC concrete.
- The optimum dosage when using PAM is 0.01% of cement content.
- The mechanical properties of the hardened concrete with the optimum dosage of PEG400 perform better than that used with the optimum dosage of PAM at the same ages.
- When mixing the two chemical curing agents used as 1.0%PEG400+0.01%PAM, the mechanical properties of SC concrete significantly improved compared to using each of PEG400 or PAM individually at all ages.

Generally, using PEG and PAM is efficient as a chemical self-curing agent to produce SC concrete with satisfied characteristics. Using a combination of PEG and PAM enhance the concrete strength with less cost as the PEG dosage decreased from 4.0% to 1.0% (which considered an expensive material) while PAM is cheaper material and its dosage is very small. That can be applied to cast self-curing concrete in poor water areas.

References

ACI.308R–01 (2001). Guide to Curing Concrete. American Concrete Institute, Farmington Hills, Detroit, USA.

Ambily PS, Rajamane NP (2007). *Self Curing Concrete: An Introduction*. [Internet]. [cited 2013 Aug 20].

ASTM.C-494 (2003). *Chemical Admixtures*. American Society for Testing and Materials ASTM International, Philadelphia, USA.

Bashandy AA (2015). Performance of self-curing concrete at elevated temperatures. *Indian Journal of Engineering & Materials Sciences*, 22, 93-104.

Bashandy AA (2016). Self-curing concrete under sulfate attack. *Archives of Civil Engineering*, 62(2), 3-18.

Bentur A, Igarashi SA, Kovler K (2001). Prevention of autogenous shrinkage in high-strength concrete by internal curing using wet lightweight aggregates. *Cement and Concrete Research*, 31(11), 1587-1591.

Chella-Gifta C, Prabavathy S, Yuvaraj-Kumar G (2013). Study on internal curing of high performance concrete using super absorbent polymers and lightweight aggregates. *Asian Journal of Civil Engineering*, 14(5), 773-781.

Dhir RK, Hewlett PC, Dyer TD (1995). Durability of self-cured concrete. *Cement and Concrete Research*, 25(6), 1153-1158.

E.C.P. 203/2007 (2007). Egyptian Code of Practice: Design and Construction for Reinforced Concrete Structures. Research Centre for Houses Building and Physical Planning, Cairo, Egypt.

E.S.S. 1109/2008 (2008). Aggregate. Egyptian Standard Specification. Ministry of Industry, Cairo, Egypt.

E.S.S. 4756-1/2009 (2009). Portland Cement, Ordinary and Rapid Hardening. Egyptian Standard Specification. Ministry of Industry, Cairo, Egypt.

El-Dieb AS (2007). Self-curing concrete: water retention, hydration and moisture transport. *Construction and Building Materials*, 21, 1282-1287.

El Dieb AS, El-Maaddawy T, Mahmoud AAM (2012). Water-soluble polymers as self-curing agents in cement mixes. *Advances in Cement Research*, 24(5), 291-299.

Emam EA (2012). Durability of Self-Curing Concrete. *M.Sc. thesis*, Faculty of Engineering, Menoufia University, Menoufia, Egypt.

Jagannadha Kumar MV, Srikanth M, Jagannadha Rao K (2012). Strength characteristics of self-curing concrete. *International Journal of Research in Engineering and Technology*, 1(1), 51-57.

Jensen OM, Lura P (2006). Techniques and materials for internal water curing of concrete. *Materials and Structures*, 39, 817-825.

Junaid SM, Saddam S, Junaid M, Yusuf K, Huzaifa SA (2015). Self-curing concrete. *International Journal of Advance Foundation and Research in Science & Engineering*, 1(Special), 1-7.

Kamal MM, Safan MA, Bashandy AA, Khalel AM (2016). The performance of normal and high strength self-curing self-compacting concretes. (*under review*).

Kholia NR, Vyas BA, Tank TG (2013). Effect on concrete by different curing method and efficiency of curing compounds. *International Journal of Advanced Engineering Technology*, 4(2), 57-60.

Kovler K, Bentur A, Zhutovsky S (2002). Efficiency of lightweight aggregates for internal curing of high strength concrete to eliminate autogenous shrinkage. *Material and Structure Journal*, 34(246), 97-101.

Mather B (2001). Self-curing concrete, why not? *Concrete International*, 23(1), 46-47.

Mousa M, Mahdy MG, Abdel-Reheem AH, Yehia AZ (2014). Mechanical properties of self-curing concrete (SCUC). *Housing and Building National Research Centre (HBRC) Journal*, 11(3), 311–320.

Rai US, Singh RK (2005). Effect of Polyacrylamide on the different properties of cement and mortar. *Materials Science and Engineering: A*, 392(1), 42-50.

Sathanandham T, Gobinath R, NaveenPrabhu M, Gnanasundar S, Vajravel K, Sabariraja G, Manoj Kumar R, Jagathishprabu R (2013). Preliminary studies of self curing concrete with the addition of polyethylene glycol. *International Journal of Engineering Research & Technology*, 2(11), 313-323.

Schlitter J, Henkensiefken R, Castro J, Raoufi K, Weiss J (2010). Development of internally cured concrete for increased service life. Joint Transportation Research Program, JTRP SPR-3211.

Sun Z, Xu Q (2008). Micromechanical analysis of polyacrylamide-modified concrete for improving strengths. *Materials Science and Engineering: A,* 490, 181-192.

Vyawahare MR, Patil AA (2014). Comparative study on durability of self cured SCC and normally cured SCC. *International Journal of Scientific Research Engineering & Technology*, 3(8), 1201-1208.

Yehia AZ (2010). Application of Self-Curing Concrete in Egypt. *Ph.D thesis*. Structural Engineering Department, Mansoura University, Mansoura, Egypt.

Challenge Journal of Concrete Research Letters

Effect of reinforcement in perforated brick arrangement for determining flexural strength and corrosion loss

Mosfeka Mahabuba Akter *, Atique Shahariar, Md. Shafiqul Islam

Department of Civil Engineering, Rajshahi University of Engineering & Technology, Rajshahi, Bangladesh

ABSTRACT

Brick masonry walls consist of the main elements that responsible for the global stability of brick masonry buildings when subjected to lateral loads such as wind and seismic forces. These elements are subjected to gravity forces, bending moments and shear forces due to the horizontal loading. The application of reinforcement increases the deformation capacity, controls the crack opening and allows a better distribution of stresses. Longitudinal reinforcements increase the flexural strength, even if they seem not to influence the shear behavior. Effectiveness of reinforcement on the increase of the resistance of brick masonry wall is highly related to the failure mode of the element. This paper shows the flexural strength of reinforced perforated brick masonry wall and weight loss of reinforcements for corrosion after a certain period of time. Several reinforce bar arrangements into the perforated brick masonry walls show the variety of possible applications.

ARTICLE INFO

Article history:
Received 29 October 2016
Revised 21 January 2017
Accepted 26 March 2017

Keywords:
Perforated brick
Rebar
Reinforced masonry wall
Strength
Corrosion

1. Introduction

Brick work strengthened by the introduction of mild steel flats, hoop iron, expanded mesh or bars is termed as reinforced brick masonry (Hossain et al., 1997). This reinforced brick masonry is capable of resisting both compressive as well as tensile and shear stress. On account of its ability to resist lateral forces, reinforced brick masonry is extensively used in seismic areas. It is essential to use first class bricks with dense cement mortar in the reinforced brick work. The reinforcement should be effectively embedded and surrounded with mortar cover of 15 to 25 cm. This is necessary to protect the reinforcement against corrosion (Cabrera, 1996).

Reinforced perforated brick masonry is frequently adopted for the construction of retaining walls especially in places where exposed brick work is necessary from architectural considerations. In another case, brick work has been restricted for compression members (Kumar, 2006).

2. Experimental Program

2.1. Preparation of specimen

During the experimental study, a total of 40 brick masonry specimens (each having dimension: 10"×10"×18") were constructed where 20 specimens (1st batch) have been used for determining strength test and other 20 (2nd batch) have been used for determining strength and corrosion in rebar. An English bond arrangement of bricks was followed giving a cross-sectional area of 10"×10". The height of the specimens was 18" achieved through 10 mm mortar thickness and by laying six bricks one after another. However, masonry with mortar bond is difficult to predict for masonry flexural bond which is generally not practical (Maroliya, 2012).

The specifications for required specimen cover minimum construction requirements for masonry structures such as requirements for materials, the placing, bonding and anchoring of masonry, the placement of grout and of reinforcement (Lumantarna et al., 2014).

* *Corresponding author*. E-mail address: mahabuba.monica@gmail.com (M. M. Akter)
ISSN: 2548-0928 / DOI: https://doi.org/10.20528/cjcrl.2017.01.002

Before using in specimen construction, bricks were kept immersed in clear water for about 24 hours and then cleaned with a cloth. The ratio of cement and sand was fixed for particular brick strength. The water-cement ratio was varied to suit the fixed cement and sand ratio. The required amount of cement and sand were measured by a cylinder type vessel. A 1000 ml plastic cylinder graduated to 10 ml was used to measure water.

To obtain the mortar mix of a certain proportion, required volumes of sand and cement were mixed in dry condition. Water was gradually added to the mixture until workability of cement and sand of different proportions comes in order to construct the specimens. The workability of concrete depends on the factors like grading and proportioning of aggregates, proportion of cement, the efficiency of mixture (Aziz, 2012).

Two pieces of required diameter rod and trowel were used to facilitate spreading of mortar in a proper thickness. Bricks were then firmly embedded on this mortar. 10 mm rebar were placed vertically through the holes of perforated bricks. The vertical joints between bricks were filled up with mortar by the help of a trowel. Alternative layers of mortar of required thickness and bricks were laid up to the six layers. Each layer contains two bricks.

A final 10 mm layer of definite proportion of mortar was placed on the top of six layers. The mortar used in the top was finished smooth with steel trowels. Finally, all the mortar joints were flushed jointed. After performing these operations, all specimens were cured for 7 days before testing (Grimm, 1975). Then 10% NaCl solution was also applied for 28 days for the 2nd batch only before testing because 2nd batch was used for determining strength as well as corrosion (difference between 1st and 2nd batch).

All the specimens were numbered for identifying before the testing. From Fig. 1, we can see the arrangement of rebars clearly where different water cement ratios were taken constant for arrangement. For example, for water cement ratio 0.3, five arrangements were made. Here, arrangement no. 4 and 5 were nearly same excepting that they generated slightly different load value due to machine fault or the position of the arrangement. Fig. 2 shows steps of constructing the specimens before testing. Fig. 3 shows the application of 10% NaCl solution on specimen's surface.

(1) (2) (3) (4) (5)

Fig. 1. Different rebar arrangements.

Fig. 2. Photos of constructing specimens for testing.

The specimens were mounted on the testing machine and centred (Haach, 2011). Typical load was applied initially at a rate of 1000 kN or 224810 lbs per minute. At this loading rate, the specimens took about 1 minute to 2 minute to fail. Gradually, the 40 specimens with different number and arrangements of rebar were broken one after another. There also be the two supports were arranged on the two sides of the specimens for determining the flexural strength of the specimens at the time of testing shown in Fig. 4. Calculation for specimen flexural strength was done by dividing the ultimate load by the area of specimen (10"x10"). Here, we used 3-point loading because load measurement was easy using the machine's crosshead position sensor (typically a digital encoder), whereas the 4-point bend test had been measured using a deflectometer. In our instrument, we had a digital encoder that's why we used 3-point loading.

(a) (b)

Fig. 3. Applying 10% NaCl solution into specimens: (a) NaCl solution on top surface; (b) Covering the specimens (for curing).

2.2. Numerical details

Out of total 40 specimens, 1st batch was made for determining flexural strength only (Table 1, Fig. 5), and 2nd batch was made for determining both flexural strength of specimens (Table 2, Fig. 6) and weight losses of rebar due to corrosion (Table 3, Fig. 7).

Fig. 5(a, b, c, d) and Fig. 6(a, b, c, d) are showing the comparison of rebar arrangements and flexural strength for strength and strength with corrosion respectively. For example, for water cement ratio 0.3, arrangement no. 1 gives higher strength than other arrangements and arrangement no. 4 and 5 give the lowest nearly values.

The reason behind this occurrence is the amount of rebar. No. 1 arrangement has 6 rebars whereas no. 4 and 5 similarly have 2 rebars. So, no. 1 arrangement needs higher value of load to break whereas no. 4 and 5 need lower value of load to break. In other cases, if we change the water cement ratio then the strength value will be changing. Generally, we know that an increase in water cement ratio reduces the value of mechanical properties and increases the workability but here, by increasing water cement ratio, we have got higher strength. This is due to high temperature reason and fault of machine.

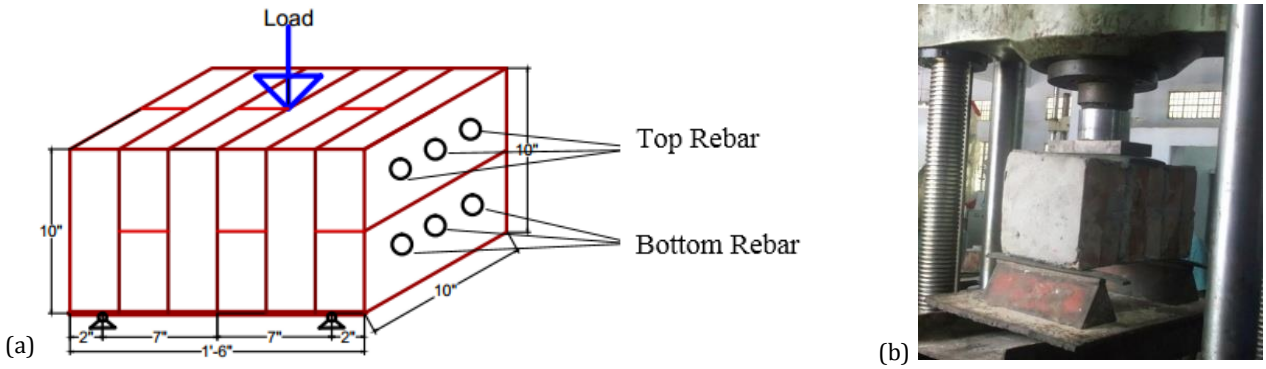

(a) (b)

Fig. 4. Testing of specimens: (a) Horizontal loading; (b) Specimens during testing.

Table 1. Flexural strength of reinforced perforated brick masonry specimens (10"x10") (for strength test only).

SL. No.	Rebar Arrangement	Water/Cement Ratio	Failure Load (kN)	Strength (psi)
1	1		67.49	151.72
2	2		53.28	119.78
3	3	0.60	46.17	103.79
4	4		39.06	87.81
5	5		36.02	80.98
6	1		64.45	144.89
7	2		51.25	115.22
8	3	0.50	45.16	101.52
9	4		37.03	83.25
10	5		35.00	78.68
11	1		61.40	138.03
12	2		44.14	99.23
13	3	0.40	40.08	90.10
14	4		36.02	80.98
15	5		32.97	74.12
16	1		58.35	131.18
17	2		41.09	92.37
18	3	0.30	39.06	87.81
19	4		33.99	76.41
20	5		30.94	69.56

** Cement/sand ratio is 1:3*

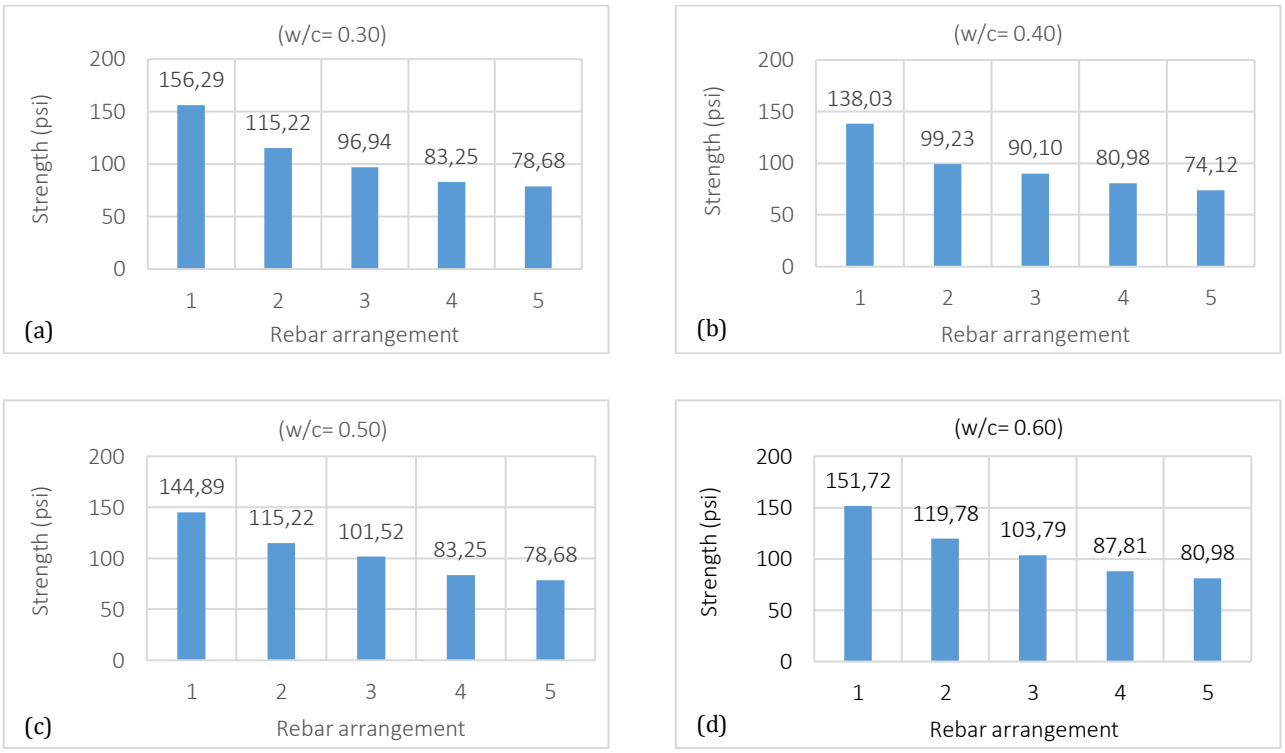

Fig. 5. Relationship between rebar arrangement and flexural strength.

Table 2. Flexural strength of reinforced perforated brick masonry specimens (10"x10") (for strength and corrosion test).

SL. No.	Rebar Arrangement	Water/Cement Ratio	Failure Load (kN)	Strength (psi)
1	1	0.30	69.52	156.29
2	2		51.25	115.22
3	3		43.12	96.94
4	4		37.03	83.25
5	5		35.00	78.68
6	1	0.40	73.58	165.42
7	2		54.29	122.05
8	3		48.20	108.36
9	4		46.17	103.79
10	5		39.06	87.81
11	1	0.50	74.60	167.71
12	2		56.32	126.61
13	3		50.23	112.92
14	4		45.16	101.52
15	5		42.11	94.67
16	1	0.60	76.63	172.27
17	2		59.37	133.47
18	3		49.22	110.65
19	4		47.19	106.09
20	5		43.12	96.94

** Cement/sand ratio is 1:3*

From Figs. 5 and 6, it is observed that the 1st arrangements have higher flexural strength with higher number of rebars. So, higher number of rebar blocks gives higher values and lower number of rebar blocks gives lesser values with the positions of rebar.

The reason behind this is the number of rebars. Specimens containing more rebars need more loads because rebar needs extra load to resist the load. In the other case, specimens containing less rebars will need less load.

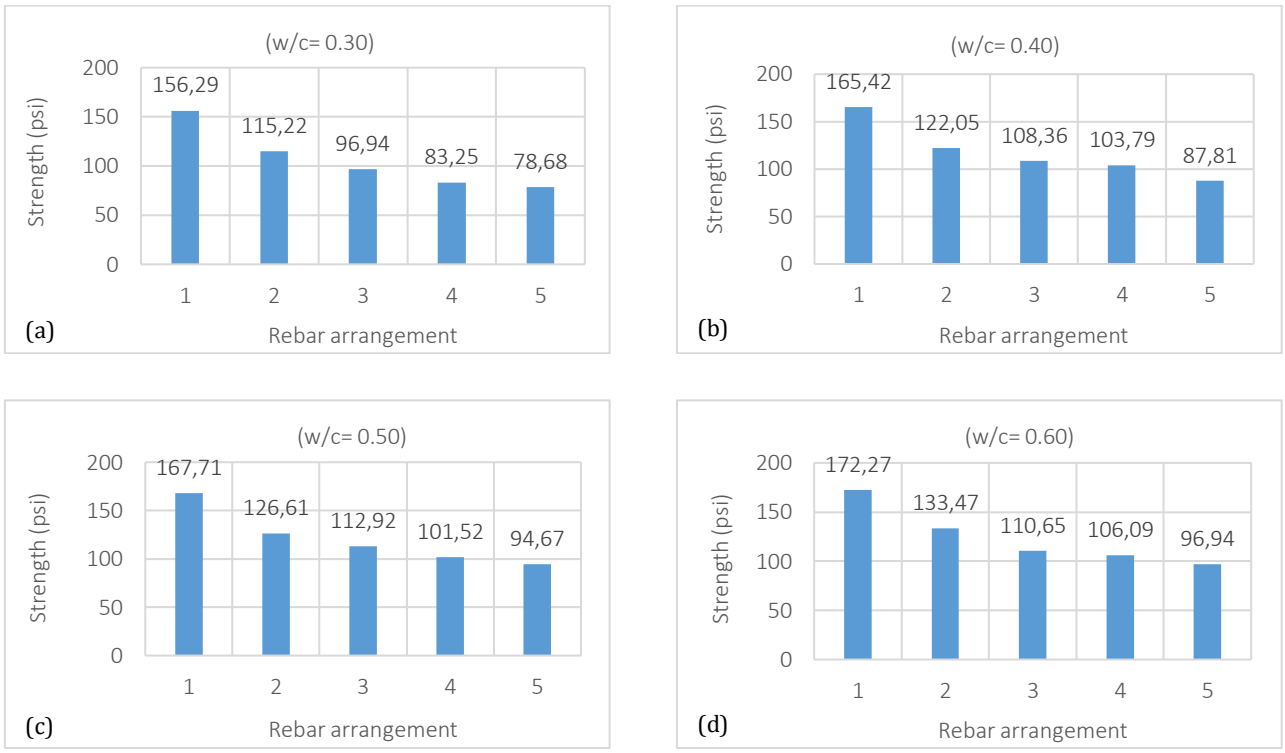

Fig. 6. Relationship between rebar arrangement and flexural strength with corrosion.

Table 3. Weight losses of rebar.

SL. No.	Rebar Arrangement	Water/Cement Ratio	% of Weight Loss (top rebar)	% of Weight Loss (bottom rebar)
1	1	0.30	0.25	0.22
2	2		0.54	0.32
3	3		0.51	0.34
4	4		0.33	0.12
5	5		0.39	0.32
6	1	0.40	0.54	0.44
7	2		0.50	0.47
8	3		0.50	0.33
9	4		0.41	0.28
10	5		0.39	0.39
11	1	0.50	0.42	0.40
12	2		0.49	0.45
13	3		0.50	0.45
14	4		0.44	0.39
15	5		0.51	0.40
16	1	0.60	0.56	0.54
17	2		0.72	0.60
18	3		0.80	0.49
19	4		0.63	0.53
20	5		0.58	0.56

3. Results and Discussion

To get accurate results, we can see the following figures (Fig. 7) where corrosion is less in arrangement no. 5. So, in fine we can say that arrangement no. 5 (for all water cement ratio: 0.3, 0.4, 0.5, 0.6) has the lowest corrosion as well as the highest strength.

From Fig. 7, it is observed that rebar arrangement 5 is comparatively less corrosive and more economical than any other rebar arrangements.

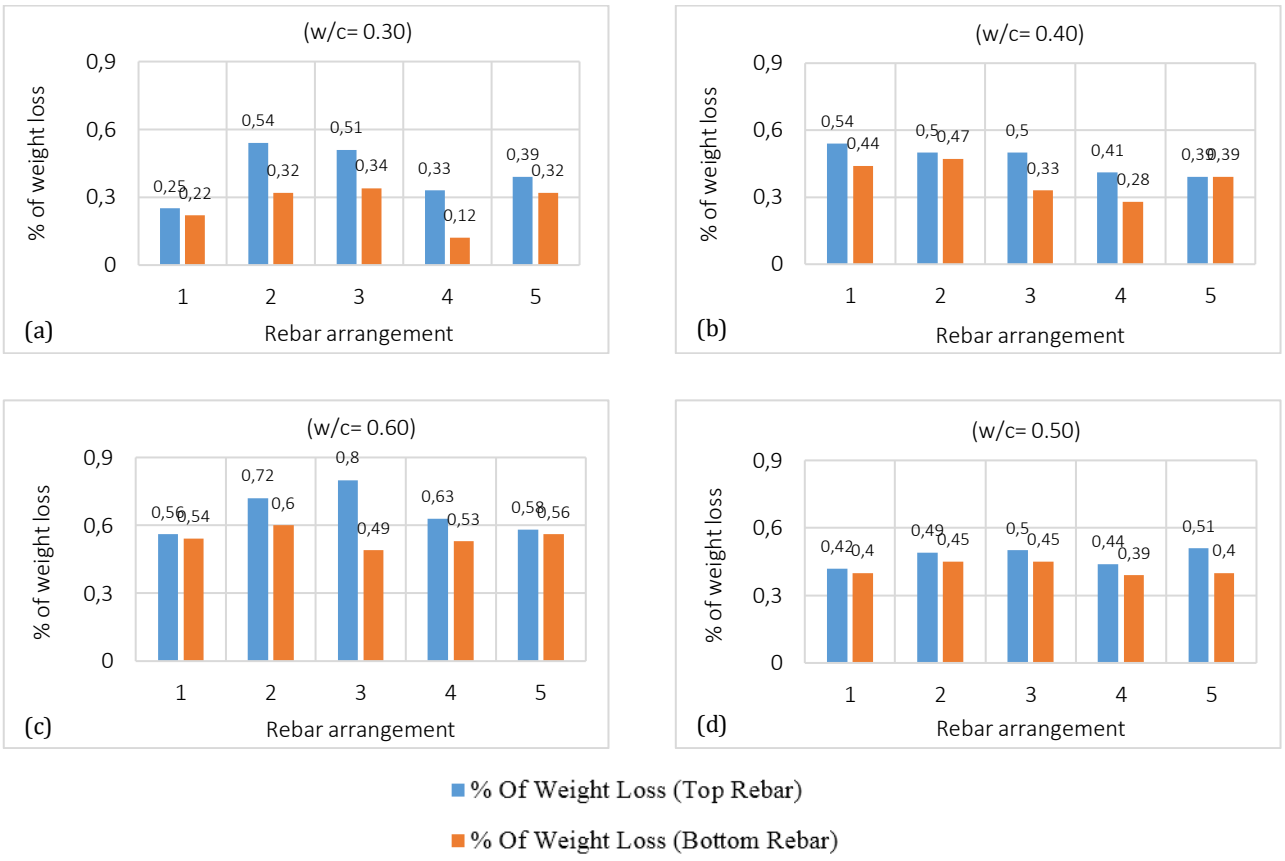

Fig. 7. Relationship between rebar arrangements and % of weight loss.

4. Conclusions

The following conclusions are drawn from the present experimental study:

- The behaviour of Reinforced Perforated Brick Masonry works to loads was observed. Arrangement 1 (6 #3 bar & w/c= 0.60) was carried the maximum flexural strength comparatively.
- Flexural strength of masonry works increases with the strength of brick, number of rebar and different rebar arrangements.
- Flexural strength of masonry works also depends on water cement ratio and mortar.

References

Aziz MAA (2012). Textbook of Engineering Materials. 1st edition, Hafiz Book Centre, Dhaka, Bangladesh.

Cabrera JG (1996). Deterioration of concrete due to reinforcement steel corrosion. *Cement and Concrete Composites*, 18(1), 47-59.

Grimm CT (1975). Strength and related property of brick masonry. *Journal of the Structural Division, ASCE*, 101(1), 217-232.

Haach VG, Vasconcelos G, Lourenço PB (2011). Parametrical study of masonry walls subjected to in-plane loading through numerical modeling. *Engineering Structures*, 33(4), 1377-1389.

Hossain MM, Ali SS, Rahman MA (1997). Properties of masonry constituents. *Journal of Civil Engineering*, The institution of Engineers, Bangladesh, 25(2), 135-136.

Kumar S (2006). Treasure of R.C.C. Designs. 14th edition, Standard Book House, Delhi, India.

Lumantarna R, Biggs DT, Ingham JM (2014). Compressive, flexural bond, and shear bond strengths of in situ New Zealand unreinforced clay brick masonry constructed using lime mortar between the 1880s and 1940s. *Journal of Materials in Civil Engineering-ASCE*, 26(4), 559-566.

Maroliya MK (2012). Behaviour of reinforced column made of hollow brick subjected to eccentric compressive load. *International Journal of Innovative Research & Development*, 1(9), 1-11.

Challenge Journal of Concrete Research Letters

Structural behavior of recycled aggregates concrete filled steel tubular columns

Boshra Eltaly *, Ahmed Bembawy, Nageh N. Meleka, Kameel Kandil

Department of Civil Engineering, Menoufia University, Shebin ElKoum, Menofia, Egypt

ABSTRACT

This paper presents an experimental and numerical investigation to determine the behavior of steel tubular columns filled with recycled aggregates concrete up to failure under constant axial compression loads. The experimental program included two steel tube columns, four recycled concrete columns and eight composite columns filled with different types of recycled coarse aggregates (granite and ceramic). Different percentages of recycled coarse aggregates: 0, 25 and 50 of the percentage of the coarse aggregates (dolomite) were used. The results of the numerical model that was employed by the finite element program, ANSYS, were compared with the experimental results. The results of the experimental study and the finite element analysis were compared with the design equations using different national building codes: AISC1999, AISC2005 and EC4. The results indicated that the recycled aggregates concrete infill columns have slightly lower but comparable ultimate capacities compared with the specimens filled with normal concrete.

ARTICLE INFO

Article history:
Received 23 January 2017
Revised 16 March 2017
Accepted 26 March 2017

Keywords:
Recycled concrete
Composite columns
Structural hollow steel
Finite element method
Buckling analysis

1. Introduction

Composite section is defined as a structural element composed of two or more different materials. These materials are joined together to act as one unit. There are several types of composite elements in civil structures; composite column, beam and slab. Many kinds of composite column have been widely used included steel-concrete (the steel may be wide-flange, box, I or any shape), steel-wood, wood-concrete, and plastic-concrete or advanced composite materials-concrete. Hollow structural (square or rectangular) steel sections are often filled with concrete to form a composite column. Such kinds of composite columns have been the interest of structural engineers because of their high load bearing capacity. In these columns, steel box (rectangular or square) plates can only buckle outward locally under compression due to the restraints of the concrete core. This buckling mode leads to a considerable increase in the critical local buckling strength of the steel box. Also the ductility of concrete core is remarkably improved because of the steel box completely encases the concrete core. Additionally using these kinds of composite columns saves the materials and speeds the construction processes because of working the steel plates as longitudinal reinforcements and permanent formworks for the concrete core (Schneider, 1998; Uy, 1998; Shanmugam and Lakshmi, 2001; Uy, 2001; Bradford et al., 2002; Sakino et al., 2004; Lam and Gardner, 2008; Chen and Jin, 2010; Liang, 2012).

Recycled Aggregates Concrete (RAC) can be recognized as a new kind of concrete construction, in which, broken pieces of waste stone, ceramic, brick or concrete are used as coarse aggregates. The physical properties of RAC depend on both adhered mortar quality and the amount of adhered mortar. The previous published researches in the field of RAC concluded that it has low strength and elastic modulus, bad workability, high water infiltration and high shrinkage and creep so that they should be only used as nonstructural concrete. Also these results indicated that recycled aggregates concrete showed similar shear crack distributions as the natural aggregates concrete. Also they indicated that natural aggregates concrete specimens had bond strengths that

* *Corresponding author*. E-mail address: boushra_eltaly@yahoo.com (B. Eltaly)
ISSN: 2548-0928 / DOI: https://doi.org/10.20528/cjcrl.2017.01.003

were 9 to 19% higher than the equivalent RAC specimens. However, RAC is well recognized in view of its low thermal conductivity, low brittleness as well as the low specific gravity that reduces the self-weight of the structures. Most importantly, the use of RAC can save natural resources and protect our living environment (Gomez-Soberon, 2002;Poon et al., 2004; Oikonomou, 2005; Etxeberria et al., 2007; Marco Breccolotti and Materazzi, 2010; Butler et al., 2011; Schubert et al., 2012; Campian et al., 2015). Evangelista and de Brito (2007) and Zega and Di Maio (2011) made concretes with recycled fine aggregates (RFA) replacing different percentages of natural river sand. Their results indicated that the compressive strengths of concretes made with 20% and 30% of recycled fine aggregates are similar to those of concrete made with 100% of natural fine aggregates.

A total of fourteen specimens were cast and tested to determine the behavior of Recycled Aggregates Concrete Filled Steel Tube Columns (RACFSTC) under axial loads up to failure. Different percentages of recycled coarse aggregates; 0, 25 and 50% of the natural coarse aggregates (dolomite) were used. The effect of composite action and the steel tube shape were studied. Their behavior includes the mode of failure, the ultimate capacity and the longitudinal strain. Also the buckling of the specimens was examined. The composite specimens were simulated by the FE program, ANSYS and their results were compared with the experimental test results. Additionally the results of the experimental study and the finite element analysis were compared with the design equations using different national building codes such as the AISC1999, AISC2005 and EC4.

2. Experimental Program

The experimental program considered four sets of test specimens giving a total of fourteen circular and square cross section columns as presented in Table 1. The specimens are with 1200 mm length, 100 mm diameter for the circular cross section specimens, 100 mm width for the box columns and 2 mm thickness as shown in Fig. 1. Their length-to-their depth and their depth-to-their tube thickness ratios remained a constant of 12 and 50; respectively. The first set of tests (S1) was designed to load the steel only and it included the control specimens; C&S specimens. The second set of tests (S2) consisted of four specimens: PC-C, R25G-C, R25C-C and R25G-C specimen and they was designed to load the concrete only and they are with circular cross section. The third set of tests (S3) was designed to load the composite section uniformly. They included four specimens; (CPC-C, CR25G-C, CR25C-C and CR25G-C). Four box columns; CPC-S, CR25G-S, CR25C-S and CR25G-S were categorized as set four (S4). In set two, set three and set four of the tests, four different types of concrete were used; plain concrete (PC100%), concrete with Recycled (R) Ceramics (C) and Granite (G) as a coarse aggregates replaced the natural coarse aggregates in plain concrete by percentage of 25% and 50% (RAC 25%G, RAC 25%C and RAC 50%G).

Table 1. Specimen details.

No. Set	Specimen Code	Specimens Designation	Concrete Code	Steel Thickness	D/t	L/D
S1	C	Circle	Empty Section	2 mm	5	12
	S	Square			5	5
S2	PC-C	Circle	PC100%	No Steel	5	12
	R25G-C		RAC25%G		5	12
	R25C-C		RAC25%C		5	12
	R50G-C		RAC50%G		5	12
S3	CPC-C	Circle	PC100%	2mm	5	12
	CR25G-C		RAC25% G		5	12
	CR25C-C		RAC25% C		5	12
	CR50G-C		RAC50% G		5	12
S4	CPC-S	Square	PC100%	2mm	5	12
	CR25G-S		RAC25% G		5	12
	CR25C-S		RAC25% C		5	12
	CR25C-S		RAC25% C		5	12

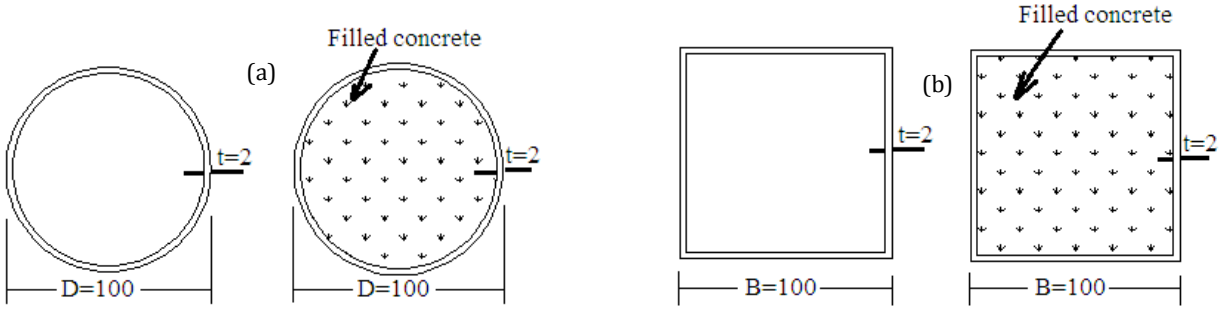

Fig. 1. Cross section details for hollow steel tube and concrete filled steel tube columns:
(a) Circular tube column; (b) Box column (all dimension in mm).

2.1. Constituent materials

The cement used was Egyptian Ordinary Portland Cement (E.S.S. 4756-1/2009). The density of the cement was 3.16 g/cm^3 and the specific surface was 3.5 cm^2/g. The chemical composition of the cement is shown in Table 2. Local sand from natural sources, clean and free from deleterious substances was used. The used coarse aggregates was commercially available (dolomite) and two RCA with different replacement percentages of the natural coarse aggregates were used; recycled ceramics and granite (Fig. 2). The physical properties of the aggregates are illustrated in Table 3. Sieve analyses were conducted for the fine and the coarse aggregates used and their results were performed and compared with the limits of the Egyptian Standard Specifications (E.S.S. 1109/2008), as shown in Tables 4 and 5; respectively. Clear water free from impurities was used for mixing. No chemical and mineral admixture was used in this study. The steel tubes are made from steel with properties indicated in Table 6.

Table 2. Chemical compositions of cement (%).

AL_2O_3	SiO_2	Fe_2O_3	CaO	MgO	SO3	k_2O	L.C.F
5.6	19.8	2.4	65.9	2.54	2.8	0.58	98.9

(a) Dolomite (b) Recycled ceramics (c) Recycled granite

Fig. 2. Natural and recycled coarse aggregates.

Table 3. Physical properties of the aggregates used.

Properties	Sand	Coarse Aggregates		
		Natural	Recycled	
			Ceramic	Granite
Mass (g/m^3)	1.73	1.75	1.55	1.7
Specific Gravity (g/cm^3)	2.6	2.7	2.6	2.7
Water Absorption (%)				1.12

Table 4. Sieve analysis of sand used.

Sieve Size (mm)	0.15	0.35	0.7	1.4	2.83	4.75
% Passing by Weight	4	15	62	79	95	100
Limits of (E.E.S.)	10-0	30-10	80-60	100-75	100-85	100

Table 5. Sieve analysis of natural and recycled coarse aggregates.

Sieve Size (mm)			2.36	4.75	9.5	12.5	20
% Limits of (E.S.S.)			5-0	15-0	70-40	100-90	100
% Passing by Weight	Natural	Dolomite	2	9	59	100	100
	Recycled	Ceramic	3	12	60	100	100
		Granite	4	14	55	100	100

Table 6. Mechanical properties of steel.

Modulus of Elasticity (GPa)	Yielding Strength (MPa)	Tensile Strength (MPa)
200	235	350

2.2. Concrete mix design

The mortar mix was designed according to Egyptian code of practice (E.C.P. 203/2007). Table 6 shows one meter cube (m^3) of the mixes. Twelve 150 x 150 x 150 mm cubes were cast and tested after 7 and 28 days, to determine the compressive strength of the matrix with the selected mortar mix. Compression test was carried out according to the E.S.S. (E.S.S. 2070/2007) on a hydraulic compression testing machine and the average strengths of the cubes are presented in Table 7. Also four 50 x 50 mm cylinders were cast and test to determine the splitting tensile stress of the mix after 28 days.

Table 7. Concrete mix and average strength for the plain concrete and recycled concrete.

Mix No.	Concrete Code	Concrete Mix (kg/m^3)					Average Strength (MPa)		
							Compression		Tension
		C	W/C %	S	NCA	RCA	7 days	28 days	
1	PC 100%	450	0.55	920	752	0	25.8	36.26	3.82
2	RAC 25%G	450	0.55	935	532	220	24	33.48	3.38
3	RAC 25%C	450	0.55	915	564	188	22.5	32.0	3.25
4	RAC 50%G	450	0.55	935	376	376	22.5	32.4	3.2

2.3. Specimens preparation

The filled concrete specimen's preparation passed through three stages. At the first stage, the steel sections were prepared. Segments with 314 mm cutting width for box columns and with 400 mm for the specimens of the square sections and 1200 mm interrupted length were cutting from steel sheet 2000 x 1200 x 2 mm total dimensions. Then each piece was formed to be with required cross section and was welded using automatic submerged welding machine. Finally, sections were settled after removing welding impurities and were painted by insulator paint to prevent corrosion of steel during treatment. At the second stage, the top and the bottom base plate were prepared as shown in Fig. 3. At the third stage, the concrete was mixed and cast in the steel section (Fig. 4). Then the column was compacted during casting. Finally, the samples were treated in the water sector until two days before the test.

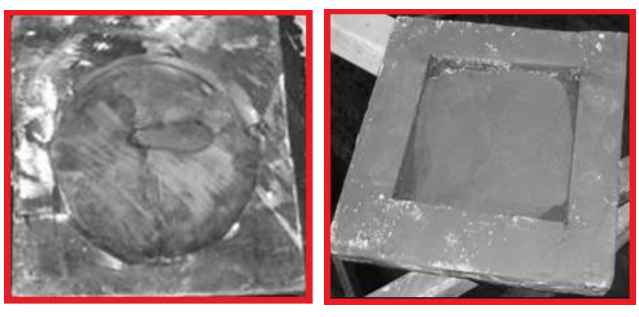

Fig. 3. Circular and box base plates.

Fig. 4. Mixing and casting concrete.

2.4. Test setup

The prepared specimen was inserted into a 5000 kN testing machine as shown in Fig. 5. Two base plates (30 mm thickness) were placed on the top and bottom ends of the specimens to ensure uniform load distribution. The loading rate was 50 kN per minute. A 2000 kN load cell was attached to the upper machine head to measure the load during testing. Two transducer springs LVDT's of length 50 mm was used to measure the lateral displacement of the tested columns as shown in Fig. 6. Two strain gauges were fixed longitudinally on the outside surface of the steel tubes to monitor the axial strain of the steel tube as illustrated in Fig. 6. All the instrumentations were connected to a data accusation system to record different measurements with a rate of recording of one reading per second.

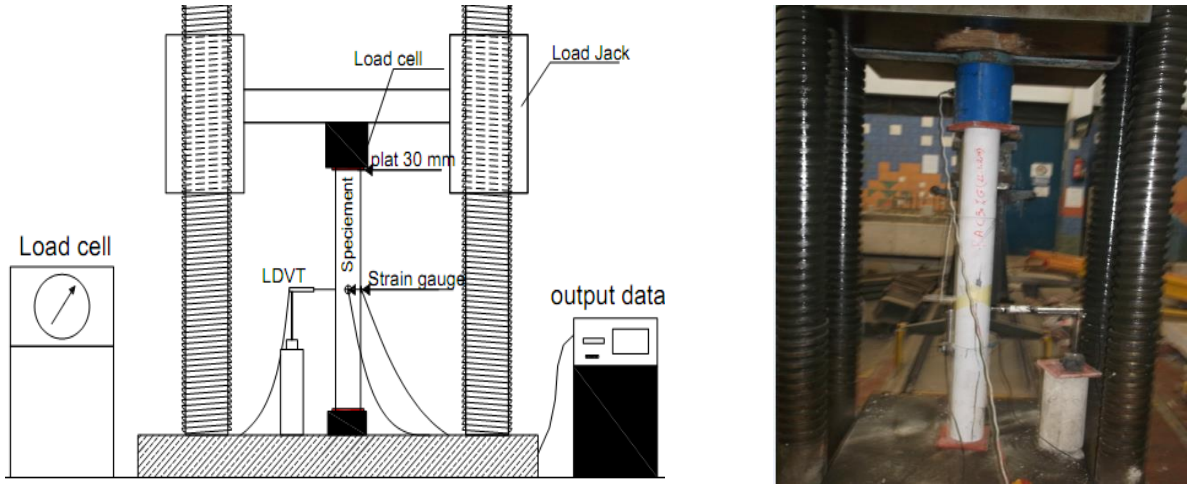

Fig. 5. Test machine and setup.

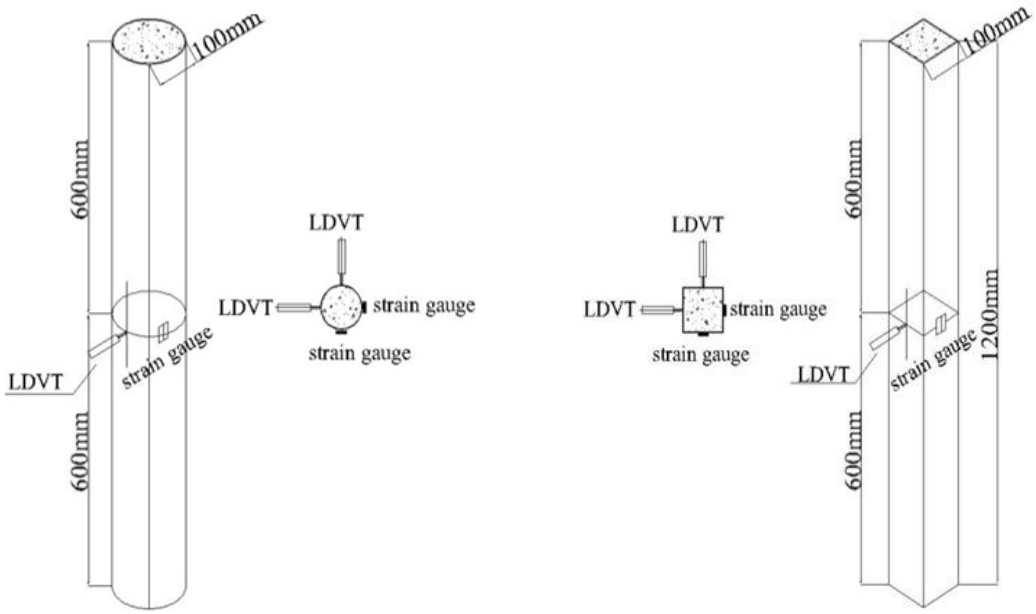

Fig. 6. Location of strain gauges and LVDTs.

3. Numerical Analysis

The composite tested columns were simulated by FE program; ANSYS 12. The current simulation model takes in consideration the geometry and the material nonlinearities. In this simulation, Soild65 elements were used for presented concrete (Fig. 7). Each element is defined by eight nodes and each node has three degrees of freedom (translations in the nodal *x*, *y*, and *z* directions). This element has cracking and crushing capabilities (ANSYS, 2006; Hoque, 2006; Singh, 2006; Aboul-Anen et al., 2009; Shaheen et al., 2013; Shaheen et al., 2014). Shell181 elements were used for modeling steel tube. Each element was defined by four or three nodes with six degree of freedoms at each node: translation in the *x*, *y*, and *z* directions and rotation about the *x*, *y*, and *z* directions as shown in Fig. 8. Shell181 element is well-suited for large rotation and large strain nonlinear applications (ANSYS, 2006; Patel and Lande, 2016). At the bottom of the column, all nodes had transition restraints in the *x*, *y*, and *z* directions. At the top of the column, perimeter nodes were restrained in *x*, *y*, and *z* directions. All other nodes were free to translate or rotate at any direction. The FE model is illustrated in Fig. 9.

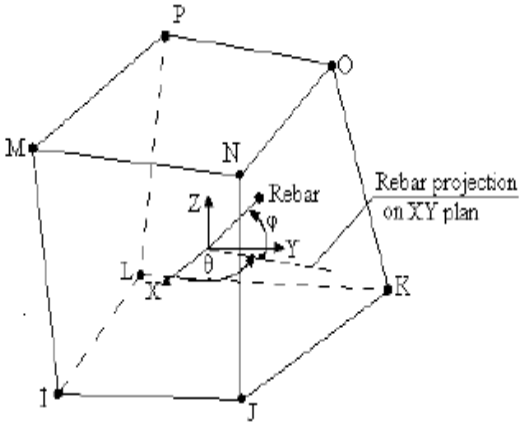

Fig. 7. Solid65 element.

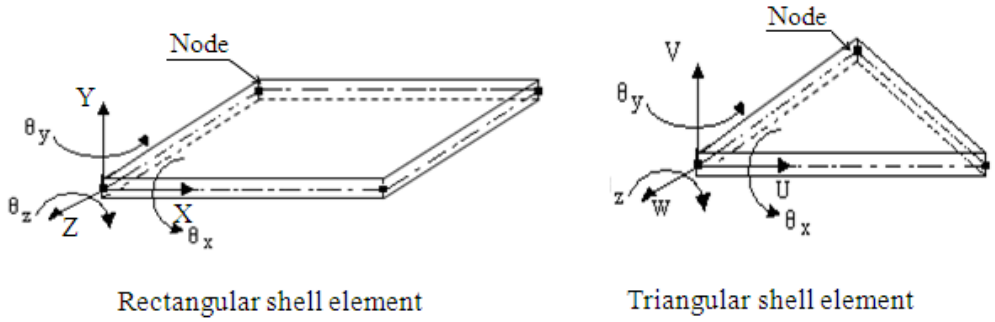

Fig. 8. Shell181 element.

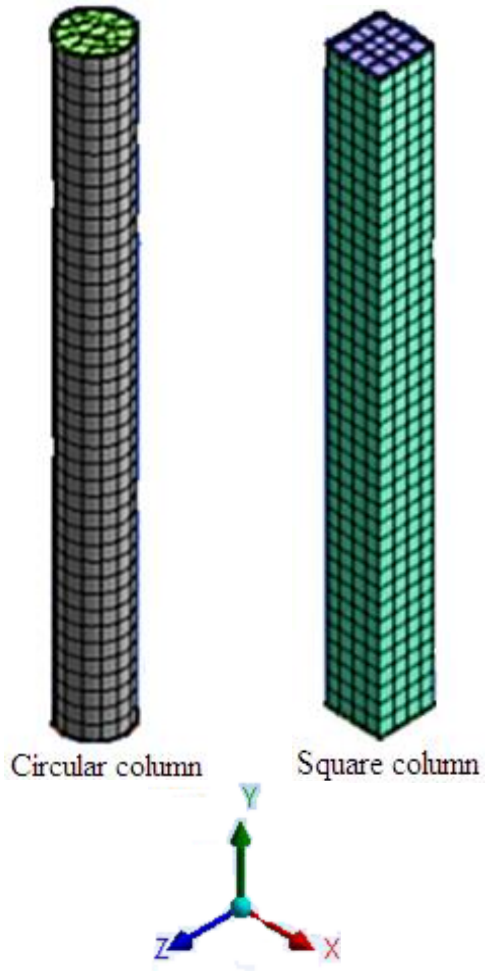

Fig. 9. FE simulation.

Cracking is permitted in three orthogonal directions at each integration point and the cracking is modeled in ANSYS program. If cracking occurs at an integration point, the cracking is modeled through an adjustment of material properties which effectively treats the cracking as a smeared band of cracks, rather than discrete cracks (Wilson et al., 1973). Also if a crack is detected at an integration point, the stress-strain relationship is modified by introducing a plane of weakness in the direction normal to the crack face. To simulate the nonlinear behavior of the specimens, the modules of elasticity, the compressive and tensile strength of concrete after 28 days and the stress-strain curve of concrete mix must be defined to the program. The modulus of elasticity of concrete and stress-strain curve were calculated according to the Egyptian Code (E.C.P. 203/2007). By considering the compressive strength of concrete after 28 days (F_{cu} in MPa), The modulus of elasticity of concrete (E_c in MPa) can be calculated from Eq. (1). The multi-linear isotropic stress-strain curve for the concrete can be computed by Eq. (2). The stress-strain curve for the unconfined concrete mix is presented in Fig. 10.

$$E_c = 4400\sqrt{F_{cu}} \tag{1}$$

$$Stress = \frac{E_c \varepsilon}{1 + (\varepsilon/\varepsilon_0)^2} \tag{2}$$

$$\varepsilon_0 = \frac{2F_{cu}}{E_c} \tag{3}$$

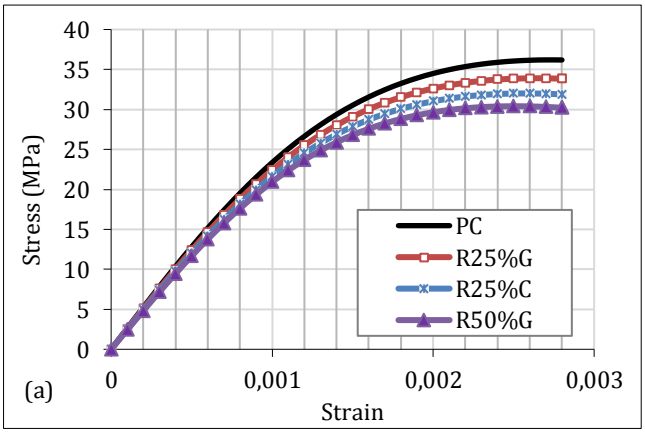

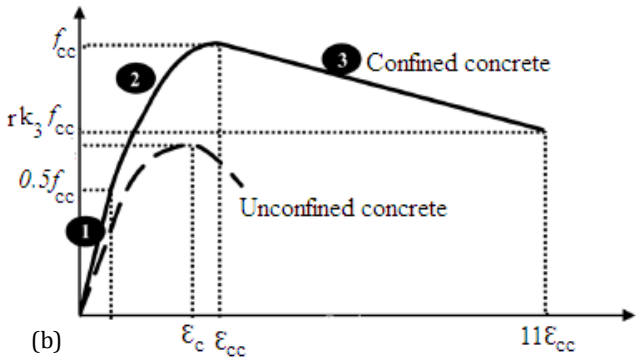

Fig. 10. Stress- strain curves for concrete used: (a) Unconfined concrete; (b) Confined concrete (Saenz, 1964).

The confinement provided by the steel tube on the concrete increases the strength and ductility of the concrete. This confinement depends on the steel depth-to thickness (D/t) ratios. A lower value of D/t ratio gives high considerable confinement for the concrete however a higher D/t ratio provides failure of the columns due to local buckling of the steel tube (Mander et al., 1988; Zuboski, 2013). The compressive strength; f_{cc} of confined concrete and the corresponding confined strain; ε_{cc} were calculated from Eqs. (5) and (6); respectively (Mander et al., 1988). Where σ_{lat} is the lateral confining pressure imposed on the concrete by the steel tube and the factors k1 and k2 were considered as 4.1 and 20.5; respectively (Patton and Singh, 2014). The stress-strain curve of confined concrete is presented in Fig. 10. The first part of the curve is the elastic part up to the proportional limit ($0.5f_{cc}$). The second part of the curve starts from the proportional limit stress ($0.5f_{cc}$) to the f_{cc}. This part was adapted from Eqs. (7-9) (Patton and Singh, 2014). R_σ is the ratio of maximum compressive strength of concrete to the stress corresponding to maximum strain on stress-strain curve. R_ε is the ratio of maximum strain on stress-strain curve to the strain corresponding to maximum compressive strength. The two factors were considered as 4.0. The third part of the curve is used to describe the softening behavior of the concrete. It starts from f_{cc} to a value lower than or equal to rk_3f_{cc} and this part does not considered in the analysis.

$$f_{cc} = f_c + k_1\sigma_{lat} \tag{4}$$

$$\varepsilon_{cc} = \varepsilon_c\left(1 + k_2\frac{\sigma_{lat}}{f_c}\right) \tag{5}$$

$$f = \frac{E_{cc}\varepsilon}{1 + (R + R_E - 2)\left(\frac{\varepsilon}{\varepsilon_{cc}}\right) - (2R - 1)\left(\frac{\varepsilon}{\epsilon_{cc}}\right)^2 + R\left(\frac{\varepsilon}{\epsilon_{cc}}\right)^3} \tag{6}$$

$$R_E = \frac{E_{cc}\,\varepsilon_{cc}}{f_{cc}} \tag{7}$$

$$R = \frac{R_E(R_\sigma - 1)}{(R_\varepsilon - 1)^2} - \frac{1}{R_\varepsilon} \tag{8}$$

The behavior of the steel tube is modeled according to the simple plastic theory (Salem, 1970; Vazirani and Ratwani, 1996). According to their theory strain hardening is neglected. The relation between the stress and strain extends from zero stress and strain passing through the linear zone to the yield (σ_y) point and finally through zero slops horizontal part of the curve. To describe this relationship into the program, the steel sheet modulus of elasticity, yield stress and tangent modulus or strain hardening modulus were defined to the program as explained in the experimental work. In the current analysis, the load-control technique was considered. In this technique, the load was applied to the model and it was divided into a series of increments called load steps. The load steps were defined by program user. After completing each increment, the stiffness matrix of the model is adjusted to reflect nonlinear changes in structural stiffness. This change occurs before proceeding to the next load increment.

The ANSYS program uses Newton-Raphson method for updating the model stiffness. The design of composite columns is addressed by a large number of design specifications. AISC-LRFD (1999), AISC-LRFD (2005) and EC4 (2004) codes were used to determine the ultimate load of composite specimens and their results were compared with the numerical and experimental results.

4. Results and Discussion

The experimental results of the ultimate failure loads for all specimens tested are presented in Table 8. Fig. 11 showed the full collapse of all specimens tested as obtained from the experimental program. The effectives of the recycled concrete in the behavior of the long columns are presented in Figs. 12 and 13. Fig. 12 shows the load-strain curves for the four circular concrete columns and Fig. 13 represents the comparison between the ultimate loads for these columns.

Figs. 14 and 15 illustrate the experimental load-strain curves and load-lateral displacement curve for S3 specimens. Fig. 11 and Table 8 illustrate that the failure occurs in steel column due to local buckling and it occurs due to concrete crushing in the concrete columns. On the other hand the failure occurs in composite columns because of global buckling in specimens with circular cross sections and local buckling in all specimens with square cross sections except that CR50G-S specimen.

From Fig. 12, it can be seen that the load-strain curves for all the four specimens of S2 group are linear till the ultimate load then the load are decreased. Also Figs. 12 and 13 and Table 8 indicate that RAC columns have slightly lower comparable ultimate capacities compared with the normal concrete specimen. The ultimate capacities of the in filled steel circular column with normal concrete were about 16 and 8 percent higher than those containing 25 and 50 percent recycled granite coarse aggregates; respectively as shown in Figs. 14 and 15 and Table 8. Also these figures indicated that the specimen with The RAC 25C% concrete mix nearly achieved the same properties as the plain concrete mix maintaining the mix proportions and its production order the same.

The effect of composite action is presented in Fig. 16. From this figure, it can be seen that the ultimate loads of composite columns are 250 percent higher than concrete or steel columns. The strain at the mid-height for specimens with square cross section are measured and given in Figs. 17-19. These Figures show that the increasing ranges of ultimate load of plain concrete column are about 11 and 17 percent. Table 8 indicates that the ultimate strength in circular section column is 30 to 40 percent higher compared to square section. This is because circular section takes confining effect better than square section.

The deformed shapes of the test columns as observed from the tests were compared with the deformed shapes obtained from the finite element analysis. It was found that good agreement exists between the experimental and numerical deformed shapes of the columns as shown in Fig. 20. The experimental and numerical ultimate load-axial strain relationships for specimen

CR50G-C as a sample are presented in Fig. 21. The comparison between the ultimate loads of composite columns as obtained from the FE simulation and four design procedures are illustrated in Tables 9 and 10 for specimens with circular and square sections; respectively.

Results in Table 9 and Table 10 show that AISC-LRFD (1999), AISC-LRFD (2005) and EC4 (2004) are conservative for predicting the member capacities of the specimens with different RAC contents. Overall, AISC-LRFD (1999) and AISC-LRFD (2005) gives ultimate capacity about 11% and 7% respectively; lower than the results obtained from the tests. However, EC4 (2004) gives capacity of the column as presented in Table 8 and Table 9 about 2% higher than those of the measured ultimate strength, and from that it can be concluded that it is an unsafe predictor. Also the two tables show that the FE simulation gives acceptable results compared to the experimental results.

Table 8. Specimens' results.

No. Set	Specimen Code	Ultimate Load P_u (kN)	Max. Strain (μ£)	Lateral Displacement (mm)	Failure Mode
S1	C	141.68	562.675	----	Local failure at the column ends
	S	154.56	1247.84	0.976	Steel local buckling
S2	PC-C	175.17	1930	---	Concrete crushing
	R25G-C	149.41	1803	---	
	R25C-C	141.86	1687	----	
	R50G-C	131.37	1597	---	
S3	CPC-C	654.3	1802.85	10.08	Global buckling
	CR25G-C	575.73	14163.5	9.109	
	CR25C-C	552.55	4003.795	4.773	
	CR50G-C	547.4	14413.2	4.334	
S4	CPC-S	604.07	2937.77	---	Steel local buckling
	CR25G-S	537.09	3754.03	----	
	CR25C-S	533.233	1612.42	-----	
	CR50G-S	504.89	1461.71	23.52	Global buckling

Table 9. Experimental and numerical of concrete filled circular steel tubular columns.

Specimen Code	$P_{Exp.}$ (kN)	FE		AISC-LRFD (1999)		AISC-LRFD (2005)		EC4 (1994)	
		P_{FE} (kN)	P_{Exp} / P_{FE}	P_U (kN)	P_u / P_{Exp}	P_U (kN)	P_u / P_{Exp}	P_U (kN)	P_u / P_{Exp}
CPC-C	654.3	595.4	1.098	590.8	0.903	602.6	0.921	635.98	0.972
CR25G-C	575.73	526.7	1.092	521.5	0.906	548.6	0.953	622.90	1.082
CR25C-C	533.233	513.8	1.075	482.8	0.88	507.5	0.925	570.64	1.04
CR50G-C	504.89	488.3	1.121	487.8	0.883	508.8	0.921	540.34	0.978
Mean	-	-	1.097	-	0.893	-	0.93	-	1.018

Table 10. Experimental and numerical ultimate loads of concrete filled square steel columns.

Specimen Code	$P_{Exp.}$ (kN)	FE		AISC-LRFD (1999)		AISC-LRFD (2005)		EC4 (1994)	
		P_{FE} (kN)	P_{Exp} / P_{FE}	P_U (kN)	P_u / P_{Exp}	P_U (kN)	P_u / P_{Exp}	P_U (kN)	P_u / P_{Exp}
CPC-S	604.7	575.1	1.053	561.2	0.927	553.9	0.915	619.8	1.024
CR25G-S	537.09	474.5	1.064	464.5	0.92	458.4	0.908	511.96	1.014
CR25C-S	534.54	475.7	1.123	500.9	0.937	494.4	0.925	552.7	1.034
CR50G-G	537.09	494.1	1.086	491.4	0.915	484.9	0.903	541.3	1.008
Mean	-	-	1.081	-	0.924	-	0.912	-	1.020

Fig. 11. Failure mode of tested specimens.

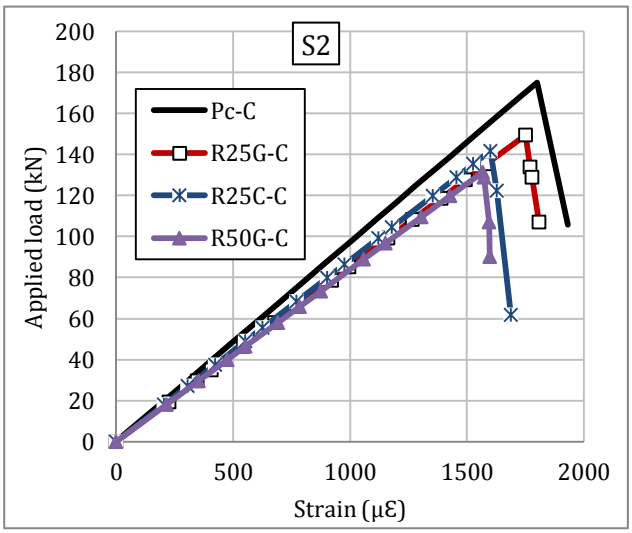

Fig. 12. Applied load-strain curve for S2 specimens.

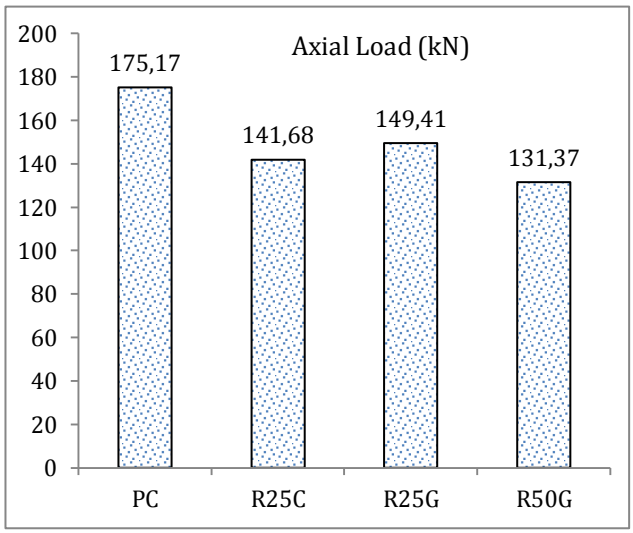

Fig. 13. Comparison between tested specimens of S2.

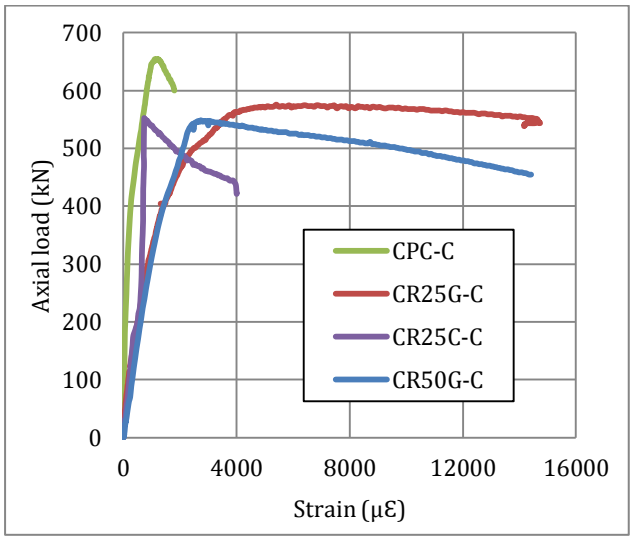

Fig. 14. Applied load-strain curve for S3 specimens.

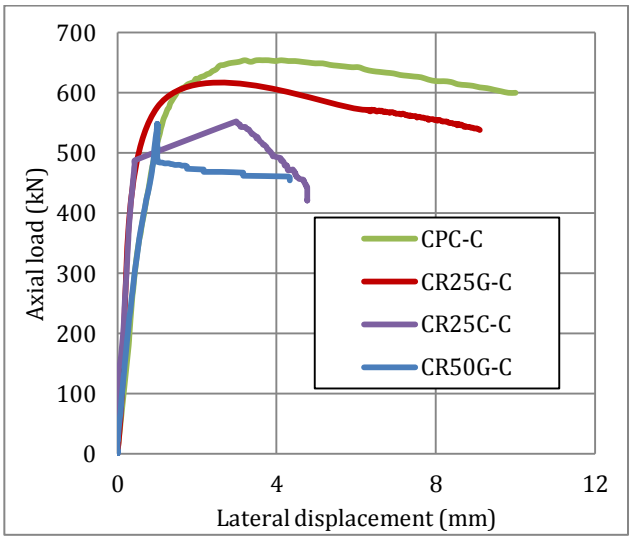

Fig. 15. Applied load-lateral displacement curve for S3 specimens.

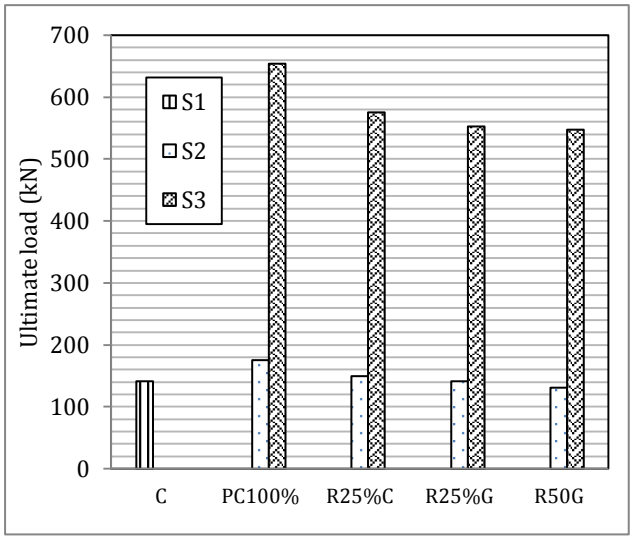

Fig. 16. Ultimate load for all circular specimens.

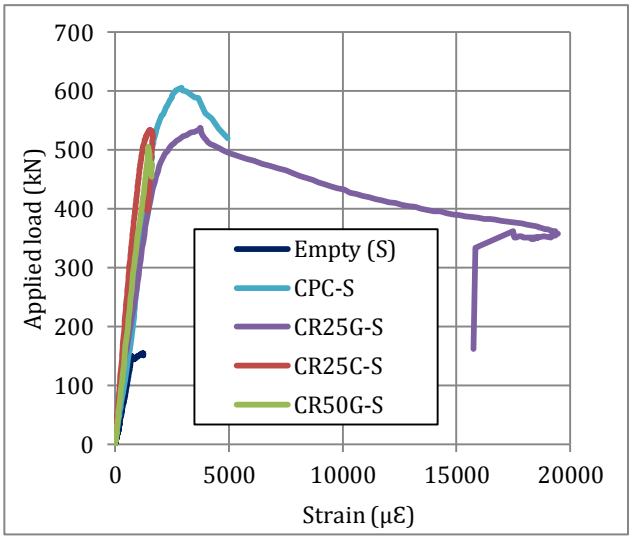

Fig. 17. Applied load-strain curve for S4 specimens.

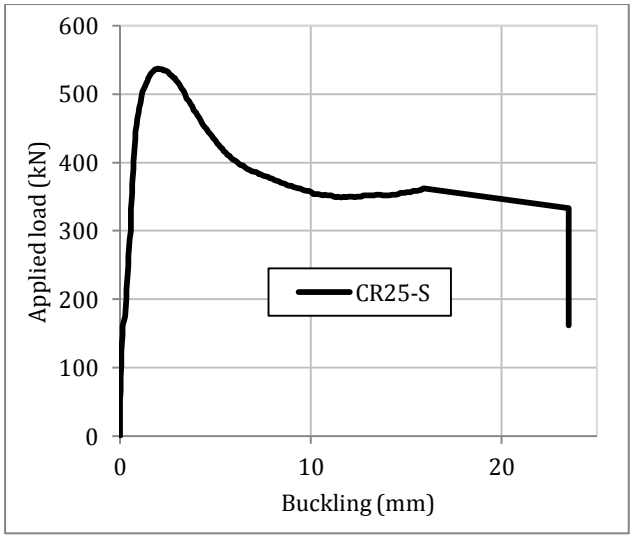

Fig. 18. Load-buckling curve of CR25-S specimens.

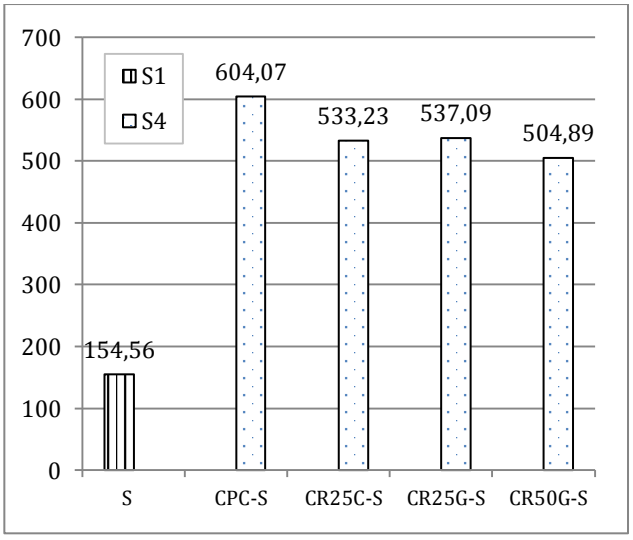

Fig. 19. Ultimate load of box column.

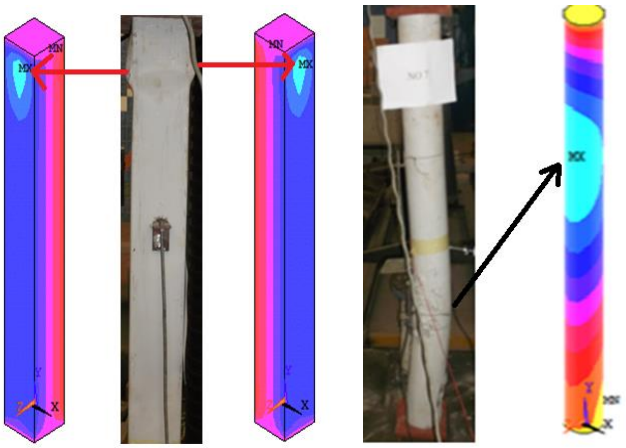

Fig. 20. Experimental and FE simulation failure modes.

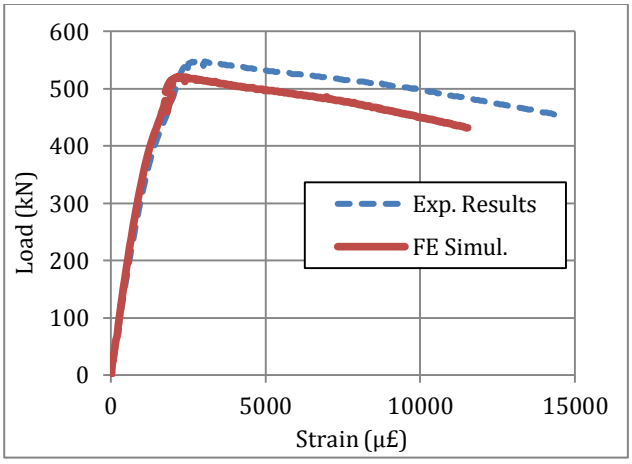

Fig. 21. Experimental and numerical load-axial strain for specimen CR50G-C as a sample.

5. Conclusions

The main objective of this study is to evaluate the structural behavior of recycled aggregates concrete-filled steel tubular columns under compression forces up to failure as well as to examine the effects of different parameters that recycled aggregates ratio, type of recycled aggregates, steel tube shape and the effect of the composite action. The study consisted of an experimental investigation, theoretical and numerical study. A total of fourteen specimens were cast and tested under compression axial loading conditions in the laboratories of the Housing and Building National Research Center, Egypt. The modes of failure, the ultimate capacities and the general deformational behavior of the specimens, based on the measured strain and buckling introduced and the cracking behavior of specimens were presented and discussed. Analytical models by finite element method were employed for the composite specimens and were compared with the experimental results. The composite specimens were also analyzed by different national building codes such as AISC-LRFD (1999), AISC-LRFD (2005) and European code EC4 (2004). Also the experimental, analytical and numerical results were compared. Based on the results of this study, the following conclusions can be drawn:

- The typical failure modes of Recycled Aggregates Concrete Filled Steel Tube (RACFST) columns are similar to those of the normal CFST columns. They were all failed due to buckling.
- The ultimate capacities of composite columns successfully increased more than 250 percent compared with concrete or steel columns.
- The recycled aggregates concrete filled columns have slightly lower but comparable ultimate capacities compared with the filled specimens with normal concrete. The ultimate capacities of the filled steel circular column with normal concrete were about 8 and 16 percent higher than those containing 25 and 50 percent recycled coarse aggregates; respectively.
- For square filled steel tube column with normal concrete, the increasing ranges are about 11 and 17 percent. The lowering in capacities of RACFST columns can be attributed to the lower strength of recycled aggregates concrete as compared to normal concrete.
- The ultimate load of columns with circular section is greater than ultimate load of columns with square section by about 30 to 40 percent. This is because circular section takes confining effect better than square section.
- It was found that, the FE model gives good results comparing with the experimental results.
- From the results of this study, it is proved that RAC has given acceptable results comparing with NPC. Moreover using RAC preserves the environment and reduces the cost of construction.
- AISC-LRFD (1999) and AISC-LRFD (2005) gives ultimate capacity about 11 and 7 percent respectively; lower than the ultimate capacity obtained from the tests.
- EC4 (2004) gives a member capacity about 1.0 to 3.4 percent higher than the experimental result for circular and square RACFST columns respectively.
- Composite specimens have given ductility failure behavior comparing with concrete and steel specimens. This leads to an early warning before complete failure occurring.

References

Aboul-Anen B, El-Shafey A, El-Shami M (2009). Experimental and analytical model of ferrocement slabs. *International Journal of Recent Trends in Engineering*, 1(6), 25-29.

AISC-LRFD (1999). Load and resistance factor design specification for structural steel buildings. American Institute of Steel Construction, Chicago, USA.

AISC-LRFD (2005). Specification for structural steel buildings. American Institute of Steel Construction, Chicago, USA.

ANSYS (2006). Help and Manual. ANSYS Inc., PA, USA.

Bradford MA, Loh HY, Uy B (2002). Slenderness limits for filled circular steel tubes. *Journal of Constructional Steel Research*, 58, 243-252.

Butler L, West JS, Tighe SL (2011). The effect of recycled concrete aggregate properties on the bond strength between RCA concrete and steel reinforcement. *Cement and Concrete Research*, 41, 1037-1049.

Campian C, Nagy Z, Pop M (2015). Behavior of fully encased steel-concrete composite columns subjected to monotonic and cyclic loading. *Procedia Engineering*, 117, 439-451.

Chen J, Jin WL (2010). Experimental investigation of thin-walled complex section concrete-filled steel stub columns. *Journal of Thin-Walled Structures*, 48, 718-724.

E.C.P. 203/2007 (2007). Egyptian code of practice: design and construction for reinforced concrete structures. Research Centre for Houses Building and Physical Planning, Cairo, Egypt.

E.S.S. 1109/2008 (2008). Egyptian standard specification for aggregates. Egyptian Standard Specification. Ministry of Industry, Cairo, Egypt.

E.S.S. 2070/2007 (2007). Egyptian standard specifications for plain and reinforcement concrete. Egyptian Standard Specification. Ministry of Industry, Cairo, Egypt.

E.S.S. 4756-1/2009 (2009). Egyptian standard specification for ordinary Portland cement. Egyptian Standard Specification. Ministry of Industry, Cairo, Egypt.

Etxeberria M, Vázquez E, Marí A, Barra M (2007). Influence of amount of recycled coarse aggregates and production process on properties of recycled aggregate concrete. *Cement and Concrete Research*, 37, 735-742.

Eurocode 4 (2004). European standard: design of composite steel and concrete structures. European Committee for Standardization, Brussels, Belgium.

Evangelista L, de Brito J (2007). Mechanical behavior of concrete made with fine recycled concrete aggregates. *Cement & Concrete Composites*, 29, 397-401.

Gomez-Soberon JMV (2002). Porosity of recycled concrete with substitution of recycled concrete aggregate; an experimental study. *Cement and Concrete Research*, 32, 1301-1311.

Hoque M (2006). 3D Nonlinear Mixed Finite-Element Analysis of RC Beams and Plates with and without FRP Reinforcement. *M.Sc. thesis*. University of Manitoba, Winnipeg, Manitoba, Canada.

Lam D, Gardner L (2008). Structural design of stainless steel concrete filled columns. *Journal of Constructional Steel Research*, 64, 1275-1282.

Liang QQ (2012). Biaxial loaded high-strength concrete-filled steel tubular slender beam-columns, Part I: Multiscale simulation. *Journal of Constructional Steel Research*, 75, 64-71.

Mander JB, Priestley MJN, Park R (1988). Theoretical stress-strain model for confined concrete. *Journal of Structural Engineering, ASCE*, 114(8), 1804-1826.

Marco Breccolotti M, Materazzi AL (2010). Structural reliability of eccentrically-loaded sections in RC columns made of recycled aggregate concrete. *Engineering Structures*, 32, 3704-3712.

Oikonomou ND (2005). Recycled concrete aggregates. *Cement & Concrete Composites*, 27, 315-318.

Patel V, Lande PS (2016). Analytical behavior of concrete filled steel tubular columns under axial compression. *International Journal of Engineering Research*, 5(Special 3), 629-632.

Patton ML, Singh KD (2014). Finite element modeling of concrete-filled lean duplex stainless steel tubular stub columns. *International Journal of Steel Structures*, 14(3), 619-632.

Poon CS, Shui ZH, Lam L, Fok H, Kou SC (2004). Influence of moisture states of natural and recycled aggregates on the slump and compressive strength of concrete. *Cement and Concrete Research*, 34, 31-36.

Sakino K, Nakahara H, Morino S, Nishiyama I (2004). Behavior of centrally loaded concrete- filled steel-tube short columns. *Journal of Structural Engineering*, 2(130), 180-8.

Salem AH (1970). Extension of stability considerations to the simple plastic theory. *The Bulletin of the Faculty of Engineering,* No. 4, Ain Shams University, Egypt.

Schneider SP (1998). Axially loaded concrete-filled steel tubes. *Journal of Structural Engineering*, 10(124), 1125-38.

Schubert S, Hoffmann C, Leemann A, Moser K, Motavalli M (2012). Recycled aggregate concrete: experimental shear resistance of slabs without shear reinforcement. *Engineering Structures*, 41, 490-497.

Shaheen YBI, Eltaly B, Abdul-Fataha S (2014). Structural performance of ferrocement beams reinforced with composite materials. *Structural Engineering and Mechanics*, 50(6), 817-834.

Shaheen YBI, Eltaly B, Kameel M (2013). Experimental and analytical investigation of ferrocement water pipe. *Journal of Civil Engineering and Construction Technology*, 4(4), 157-167.

Shanmugam NE, Lakshmi B (). State of art report on steel-concrete composite columns. *Journal of Constructional Steel Research*, 57, 1041-80, 2001.

Singh G (2006). Finite Element Analysis of Reinforced Concrete Shear Walls. *M.Sc. thesis*. Deemed University, India.

Uy B (1998). Local and post-local buckling of concrete filled steel welded box columns. *Journal of Constructional Steel Research*, 47, 47-72.

Uy B (2001). Strength of short concrete filled high strength steel box columns. *Journal of Constructional Steel Research*, 57, 113-134.

Vazirani VN, Ratwani MM (1996). Analysis of Structures. Textbook for Engineering Students, Khanna Publishers, China.

Wilson EL, Taylor RL, Doherty WP, Ghaboussi J (1973). Incompatible Displacement Models. *In: Numerical and Computer Methods in Structural Mechanics*. Academic Press, Inc., New York and London, 43-57.

Zega CJ, Di Maio AA (2011). Use of recycled fine aggregate in concretes with durable requirements. *Waste Management*, 31(11), 2336-2340.

Zuboski GR (2013). Stress-strain behavior for actively confined concrete using Shape Memory Alloy Wires. *Ph.D thesis*. The Ohio State University, Columbus, USA.